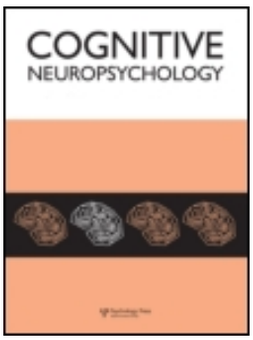

Cognitive Neuropsychology

ISSN: 0264-3294 (Print) 1464-0627 (Online) Journal homepage: http://www.tandfonline.com/loi/pcgn20

Simulating posterior parietal damage in a biologically plausible framework: Neuropsychological tests of the search over time and space model

Eirini Mavritsaki , Dietmar Heinke , Gustavo Deco & Glyn W. Humphreys

To cite this article: Eirini Mavritsaki , Dietmar Heinke , Gustavo Deco & Glyn W. Humphreys (2009) Simulating posterior parietal damage in a biologically plausible framework: Neuropsychological tests of the search over time and space model, Cognitive Neuropsychology, 26:4, 343-390, DOI: 10.1080/02643290903424329

To link to this article: http://dx.doi.org/10.1080/02643290903424329

Published online: 10 Dec 2009.

COGNITIVE NEUROPSYCHOLOGY, 2009, 26 (4), 343–390

Psychology Press
Taylor & Francis Group

Simulating posterior parietal damage in a biologically plausible framework: Neuropsychological tests of the search over time and space model

Eirini Mavritsaki and Dietmar Heinke
Behavioural Brain Sciences, School of Psychology, University of Birmingham, Birmingham, UK

Gustavo Deco
Institucio Catalana de Recerca i Estudis Avancats (ICREA), Universitat Pompeu Fabra, Computational Neuroscience, Barcelona, Spain

Glyn W. Humphreys
Behavioural Brain Sciences, School of Psychology, University of Birmingham, Birmingham, UK

The search over time and space (sSoTS) model attempts to simulate both the spatial and the temporal aspects of human visual search using spiking level neurons, which incorporate some biologically plausible aspects of neuronal firing. The model contains pools of units that (a) code basic features of objects, presumed to reside in the ventral visual stream, and (b) respond in a feature-independent way to stimulation at their location, presumed to operate in the posterior parietal cortex. We examined the effects of selective lesioning neurons responding to one side of the location map. Unilateral damage introduced spatial biases into selection that affected conjunction more than single-feature search. In addition, there was an impaired ability to segment stimuli over time as well as space (e.g., in preview search). These results match previously reported data on patients with posterior parietal lesions. In addition we show that spatial biases in selection increase under conditions in which there is decreased activity from excitatory neurotransmitters, mimicking effects of reduced arousal. Further simulations explored the effects of time and of visual grouping on extinction, generating predictions that were then tested empirically. The model provides a framework for linking behavioural data from patients with neural-level determinants of visual attention.

Posterior parietal damage and visual selection

Damage to the posterior parietal cortex (PPC) is classically associated with problems in visual selection (Critchley, 1953), including clinical deficits such as Balint's syndrome (after bilateral lesions), unilateral neglect, and extinction (after unilateral lesions). These deficits affect visual search through both space and time. For

Correspondence should be addressed to Eirini Mavritsaki, Behavioural Brain Sciences, School of Psychology, University of Birmingham, Birmingham B15 2TT, UK.

This work was supported by grants from the Biotechnology and Biological Sciences Research Council (BBSRC), Medical Research Council (MRC), and Stroke Association (UK).

http://www.psypress.com/cogneuropsychology DOI:10.1080/02643290903424329

example, serial search through space is impaired after PPC damage, evidenced by PPC patients finding it difficult to find a conjunction target or a target defined by a low-saliency single-feature difference relative to distractors (see Eglin, Robertson, & Rafal, 1989; Friedman-Hill, Robertson, & Treisman, 1995; Riddoch & Humphreys, 1987, for data on conjunctions; see Humphreys & Price, 1994; Humphreys & Riddoch, 1993), for evidence from search for single-feature-defined targets). Such patients also show deficits under conditions where visual stimuli are segmented over time. In preview search one set of distractors is temporarily segmented from the other distractors and the search target (e.g., blue Hs may appear before a new green H target and green A distractors). Even though targets can be derived by combining the features of the distractors (i.e., targets are conjunction), normal participants can detect targets under preview conditions as efficiently as in single-feature search (Humphreys, Olivers, & Yoon, 2006b; Olivers & Humphreys, 2004). This deficit that PPC patients have for preview search is not due simply to a loss of sensitivity to the transient properties of the new search stimuli (though see Batelli, Cavanagh, & Thornton, 2003), since the patients can show relatively normal effects of sudden onsets capturing attention (Humphreys et al., 2006b). Based on onset capture by the new items, preview search should be relatively efficient. Instead there seems to be a specific deficit in using the temporal separation between successive displays to bias search away from old distractors.

After unilateral damage, PPC patients often manifest a spatial bias in selection, finding it particularly difficult to attend to targets on the contralesional side of space. This is most clearly illustrated in the disorder of unilateral neglect (Bisiach & Vallar, 2000), but it is also apparent in visual extinction, when patients fail to detect a contralesional item specifically under conditions in which competing information is presented on the ipsilesional side (Karnath, 1988). Such extinction effects can be attributed to the lesion biasing attentional competition, so that ipsilesional stimuli attract more "attentional weight", winning any competition for selection (cf. Bundesen, Habekost, & Kyllingsbaek, 2005; Duncan, Humphreys, & Ward, 1997). This is consistent with the PPC reflecting the "attentional weight" being allocated to stimuli at different spatial locations (cf. Bundesen et al., 2005).

Despite these deficits in visual selection, patients with PPC damage remain able to process visual stimuli presented on the side of space contralateral to their lesion, even when the patients deny the presence of the contralesional event. For example, there is now a substantial literature demonstrating that visual extinction can be modulated by grouping between stimuli, suggesting that the contralesional stimuli can enter into grouping relations with other items in the field (e.g., Brooks, Fahey, & Kenneth, 2005; Gilchrist, Humphreys, & Riddoch, 1996; Humphreys, 1998; Mattingley, Davis, & Driver, 1997; Riddoch, Humphreys, Edwards, Baker, & Willson, 2003; Ward, Goodrich, & Driver, 1994). This is consistent with stimuli being processed (and grouping taking place) through brain regions that remain unlesioned (e.g., ventral visual cortex) in the patients, even if the PPC lesion may modulate activity in more ventral visual areas (see Rees, Backus, & Heeger, 2000, for evidence from functional magnetic resonance imaging, fMRI).

It should also be noted that not only do patients with unilateral PPC lesions manifest problems in selecting stimuli on the contralesional side of space, but they can also show impairments in selection on their ipsilesional side. For example, patients can neglect items on their ipsilesional side when cued to attend to the contralesional field (Robertson, 1994). In addition, Husain and colleagues (Husain, Shapiro, Martin, & Kennard, 1997) have demonstrated a prolonged attentional blink for stimuli presented at fixation, and Duncan et al. (1999) have reported reduced processing capacity for ipsilesional items. Hence there can be nonspatial as well as spatial deficits linked to unilateral PPC lesions. There are also clear demonstrations that ipsilesional items can abnormally increase their saliency (Ladavas, Petronio, & Umilta, 1990; Snow & Mattingley,

2006), altering the way in which these stimuli are selected in patients relative to control participants. These nonspatial deficits after unilateral PPC damage have been linked both to imbalances in spatial competition for selection (e.g., in cases of ipsilesional "capture") and to the presence of additional functional deficits, including impaired visuospatial working memory (Husain et al., 2001; Wojciulik, Husain, Clarke, & Driver, 2001) and impaired arousal (Robertson & Manley, 1999). Indeed impairments in arousal and sustained attention are important predictors of the degree of clinical deficit in neglect patients (Husain & Rorden, 2003), and spatial neglect can be reduced by temporarily increasing nonspatial, phasic arousal (Robertson, Mattingley, Rorden, & Driver, 1998). Posner and Petersen (1990), for example, propose that damage to the right PPC can disrupt the operation of the neurotransmitter systems within the right hemisphere modulating arousal. The consequence is that patients can have a conjoint problem both in spatial selection and in aspects of nonspatial selection particularly dependent on maintained arousal. This account provides one analysis of why there is a greater incidence of neglect after right than after left-hemisphere lesions (Bisiach & Vallar, 2000).

Computational modelling

As the above discussion indicates, damage to the PPC can lead to a variety of spatial and nonspatial processing disorders, with syndromes such as visual neglect associated with a wide variety of symptoms that may vary across patients and even across different occasions in the same patient. This makes it difficult to develop a detailed account of the disorders without simulating how patterns of behaviour can emerge from interactions between modules in a damaged system. Consequently, it is useful to develop explicit models of such disorders, which can provide a framework for understanding how the complex behavioural syndromes arise. Attempts to simulate neuropsychological disorders associated with PPC damage, such as unilateral neglect and extinction, have been carried using connectionist models that approximate neuronal functions at relatively high levels (see Ellis & Humphreys, 1999). These models have been able to capture a wide set of symptoms ranging from the basic disparity in spatial selection through to the influence of grouping and top-down knowledge on reducing extinction and neglect (e.g., Heinke, Deco, Zihl, & Humphreys, 2002; Heinke & Humphreys, 2003; Mozer & Behrmann, 1990; Mozer, Halligan, & Marshall, 1997; Pouget & Sejnowski, 1997). For example, Heinke and Humphreys (2003) simulated PPC damage in their selective attention for identification model (SAIM) by reducing the connectivity between units on one side of a "selection network". The selection network acted to gate the transmission of activity from the model's retina through to a "focus of attention". Damage to parts of the selection network receiving input from one side of space led to a retinotopic disorder in which stimuli on the affected side of the retina tended to lose out in any competition for mapping into the focus of attention. Damage to connections leading out from the selection network into one side of the focus of attention resulted in an object-based disorder in which elements on one side of the selected object tended to be neglected. However, the spatial biases introduced by these lesions could be reduced by top-down activity into the selection network. For example, when the item on the lesioned side coactivated a stored memory with a stimulus falling on the nonlesioned side of the selection network, top-down activation from the memory representation could enable the lesioned item to be reported. This effects a kind of grouping based on stored memory relationships between items. The model could also generate seemingly paradoxical results where the same patient can show neglect for different aspects of their environment on opposite sides of space. Humphreys and Riddoch (1994, 1995) reported a patient who, after suffering bilateral damage, showed right neglect of stimuli in retinotopic space along with neglect of the left parts of objects. Heinke and Humphreys (2003) simulated this by damaging connections between units in the selection network responding to the right side of

the retina along with connections between units connecting to the left side of the focus of attention. The simulation shows that these opposite patterns of neglect can emerge within a single framework.

Now, while connectionist models can have many virtues, they also have some limitations. For example, many such models incorporate learning through back propagation, which is not biologically realistic (see Sejnowski, 1986) and which can give rise to network properties divorced from real neuronal structures (e.g., with units acting in both an excitatory or an inhibitory manner, depending on the sign of their connection to other units). Also, many models use simplified activation functions, modified by single parameters (e.g., Servan-Schreiber, Printz, & Cohen, 1990), and so they typically fail to capture more complex neural modulations generated through different neurotransmitter systems in the human brain. In addition, many connectionist models do not have units operating in a time-based manner that can be explicitly related to the time course of neuronal processes. In such cases, time course functions must be matched to human data either in a purely qualitative manner (e.g., Heinke & Humphreys, 2003) or in time by fitting a measure based on network iterations to one based on real time (e.g., Seidenberg & McClelland, 1989). These limitations become important when we wish to simulate neurological disorders at a finer grained level, where, for example, we wish to model quantitatively the effects of varying the temporal intervals between stimuli along with variations in neuronal-transmitter signals. For example, do nonspatial deficits emerge after unilateral lesioning if there is concurrent alteration in neurotransmitter modulation (cf. Malhotra, Parton, Greenwood, & Husain, 2005)? To capture such effects, it is possible to use models that incorporate some of the biological parameters of real neuronal operations, including values representing the time course of neurotransmitter operations and of spiking activity in real neuronal systems.

Deco and colleagues (Deco & Rolls, 2005; Deco & Zihl, 2001) have simulated human attention using models based on "integrate and fire" neurons, which utilize biologically plausible activation functions and output in terms of neuronal spikes. These authors showed that a model with parallel processing of the input through to high levels simulated classic "attentional" (serial) aspects of human search (e.g., contrasting search when targets are defined by simple features with search when targets are defined by conjunctions of features; cf. Treisman & Gelade, 1980), providing an existence proof that a model incorporating details of neuronal activation functions could capture aspects of human visual attention.

The Deco and Zihl (2001) model, which forms the starting point for our own simulations (below), used a "mean-field approximation" to neuronal function, where the actual fluctuating induced local field u_i for each neuron i was replaced by its average, and so the model does not capture dynamic operations at the level of individual neurons as, for example, levels of neurotransmitter vary. Recently we elaborated this account at the level of individual neurons to simulate human spatial and temporal selection. This model, the spiking search over time and space (sSoTS) model (Mavritsaki, Heinke, Humphreys, & Deco, 2006, 2007), uses a system of spiking neurons modulated by NMDA, AMPA, GABA transmitters along with a I_{AHP} current, as originally presented by Brunel and Wang (2001; see also Deco & Rolls, 2005). The architecture of the model is illustrated in Figure 1. sSoTS uses a simplified form of feature coding, with two layers of feature maps to encode the characteristics of visual stimuli (their colour and shape). There is in addition a "location map" in which units respond to the presence of any feature at a given location. At each location (in the feature maps and the location map), there is a pool of spiking neurons, providing some redundancy in the coding of visual information. Based on the network architecture and behaviour we can think of the feature maps as corresponding to neurons in ventral cortex (e.g., V4) while the location map may correspond to neurons in dorsal (posterior parietal) cortex (though the precise details of neurons in these regions are not modelled at this stage). There are inhibitory interactions across different pools within each of the feature

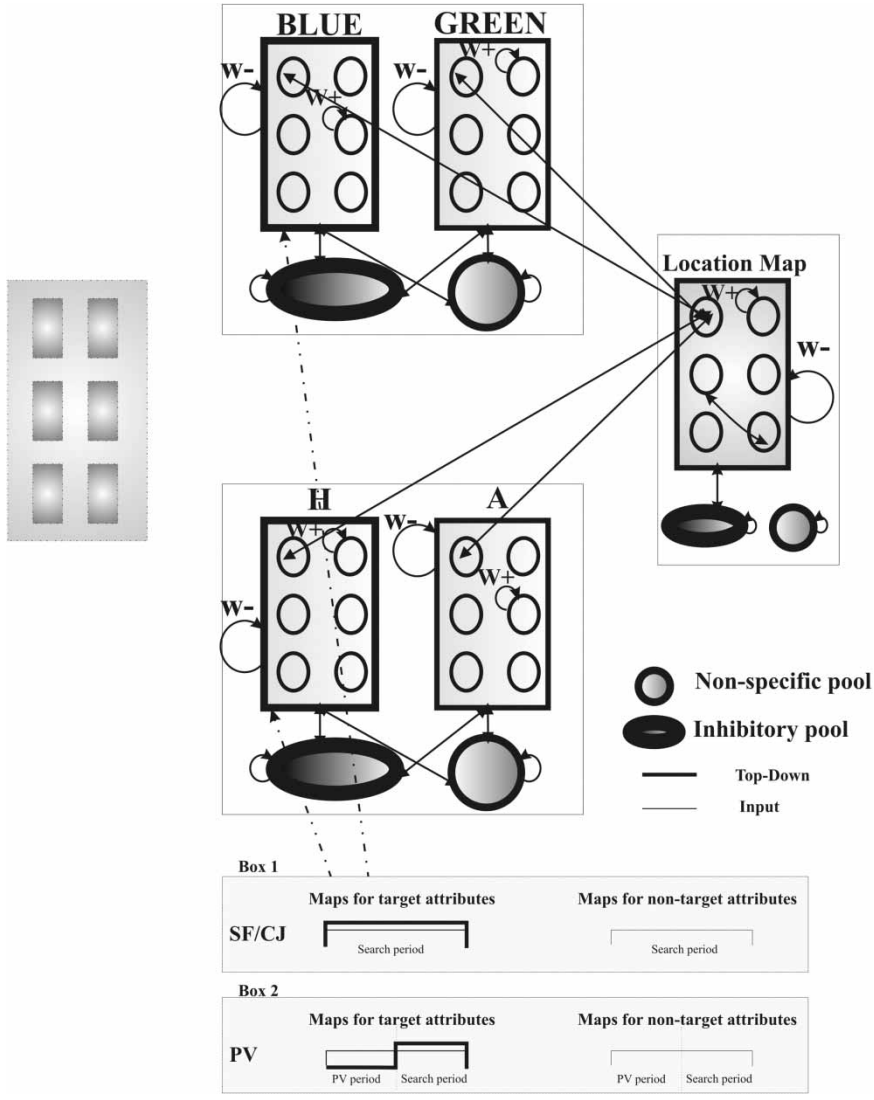

Figure 1. *The architecture of the search over time and space (sSoTS) model. The neurons within the same location pool are strongly connected (see w^{+}), and neurons in different location pools are not (see w^{-}). Each feature and location map receives global inhibition from the inhibitory pool. Furthermore, each position within the location map is reciprocally connected with the corresponding position in the feature maps. The dotted lines indicate the top-down inhibition applied to the features and locations of distractors during the preview period. At the bottom of the figure we show the time periods for the displays: single feature (SF), conjunction (CJ), and preview (PV).*

maps, modulated by a global inhibitory parameter, which represents a form of lateral inhibition between like elements. There are also inhibitory interactions between pools corresponding to the same location in different feature maps in the same feature domain (e.g., between blue and green units for Location 1, but not between, say, blue and H-shape units for Location 1), so that a given location will tend to support only one feature value within a domain. Search is simulated by giving additional activity into the feature maps corresponding to the properties of the target; this

corresponds to an expectation of the target. This activity combines with activity from the stimuli presented in the search display, and the output from each pool of neurons in each feature map is fed-forward into the map of locations. Activity in the location map provides an index of "saliency" irrespective of the feature values involved (cf. Itti & Koch, 2000), since the location units represent the strength of evidence for "something" occupying each position, but they are "blind" to the features present (which are summed across the feature maps). There is then also feedback activation from the pool of units corresponding to each position in the map of locations to units at the corresponding location in the feature maps. This "sharpens" the competition between the features. Through these competitive interactions, the location map over time comes to represent a single "winner", based on bottom-up differences between the feature values of the stimuli and top-down influences from the expectancy for target features. The time for competition to be resolved within the location map, based on the real-time operation of the neurons, can be taken as the reaction time (RT) to detect a target. Note that the real-time coding of the neurons distinguishes the model from many connectionist simulations, where RTs are based on fitting a function to translate from network iterations to RT (cf. Seidenberg & McClelland, 1989). This is also an important factor in simulating human search over time, under preview conditions (see below).

Search efficiency in sSoTS is determined by the degree of overlap between the features of the target and those of distractors, with RTs lengthening as feature overlap increases, which generates increased competition for selection. Consequently, search for a conjunction target (having no unique feature and sharing one feature with each of two distractors) is more difficult than search for a feature-defined target (differing from the distractors by a unique feature). Like Deco and Zihl (2001), Mavritsaki et al. (2006, 2007) showed that search in the conjunction condition also increased linearly as a function of the display size, mimicking "serial" search in a model operating in a purely parallel manner.

In addition to modelling spatial aspects of search, sSoSTs can also successfully simulate data on human search over time, in the preview search paradigm. The data indicate that there is a surprisingly long time course to preview search, with the interval between the initial items and the search display needing to be 450 ms or so for efficient search to emerge (Humphreys, Olivers, & Braithwaite, 2006a; Humphreys et al., 2006b; Watson & Humphreys, 1997; see Watson, Humphreys, & Olivers, 2003, for a review). The sSoTS model generates efficient preview search but also requires there to be a relatively long interval between the initial preview and the final search display. The sSoTS mimics this time course due to the contribution of two processes: (a) a spike frequency adaptation mechanism generated from a slow $[Ca^{2+}]$-activated K^+ current, which reduces the probability of spiking after an input has activated a neuron for a prolonged period (Madison & Nicoll, 1984), and (b) a top-down inhibitory input that forms an active bias against known distractors. The slow action of frequency adaptation simulates the time course of preview search using a biologically plausible parameter setting. The top-down inhibitory bias matches data from human psychophysical studies where the detection of probes has been shown to be impaired when they fall at the locations of old, ignored distractors (Agter & Donk, 2005; Allen & Humphreys, 2007; Humphreys, Jung Stalmann, & Olivers, 2004; Watson & Humphreys, 2000). In addition, in explorations of the parameter space for sSoTS, Mavritsaki et al. (2006, 2007) found that top-down inhibition was a necessary component to approximate the behavioural data on preview search (see Figure 2). These results, using the sSoTS model, indicate that processes of cooperation and competition based on local processing dynamics within the framework set out by Deco and Zihl (2001) units may not be sufficient to account for the full range of data on human selective attention and that factors such as frequency adaptation and top-down biases against distractors are required in order to simulate the temporal dynamics of visual attention.

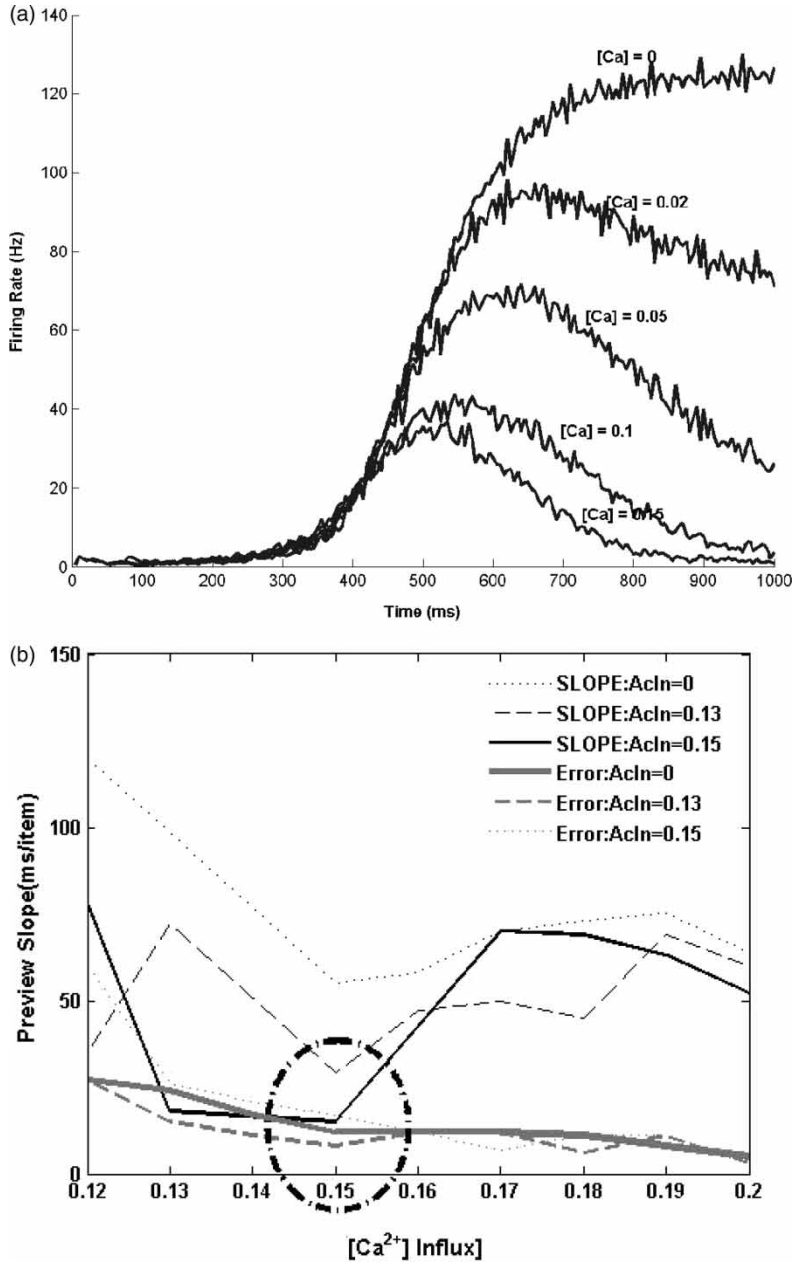

Figure 2. *(a) Illustration of variations in the neuronal firing rate as a function of the Ca^{2+} parameter. In each case there is an increase in the concentration of Ca^{2+} entering the cell after the neuron spikes, leading to increasing inhibition of the neuron and a decrease in the firing rate (frequency adaptation); altering the Ca^{2+} parameter changes the rate of this adaptation process. (b) Illustration of the search of the parameter space for search over time and space (sSoTS) as a function of two of its critical parameters, Ca^{2+} and top-down inhibition against distractor features. The parameters are fit to generate search slopes in the standard range found for human participants carrying out preview search using displays such as those employed by Watson and Humphreys (1997). The figure illustrates that the presence of an appropriate level of active inhibition helps the model to achieve search slopes in the required range. Note that, once the parameters are found to approximate human search efficiency under preview conditions, the parameters are then set for all subsequent simulations.*

In the present paper we use the sSoTS model to simulate the effects of PPC damage on human visual selection. The modelling results are presented in two sections. In Section 1 we compare the performance of sSoTS after lesioning to existing data demonstrating qualitative differences in patients across conditions of single-feature, conjunction, and preview search. The search conditions approximate those used by Watson and Humphreys (1997) and Olivers and Humphreys (2004). In Section 2 we derive two new sets of predictions from the lesioned version of sSoTS based on the effects of similarity between items and the time course of selection as item presentations vary. These predictions were then tested empirically in Section 3 by examining the performance of PPC patients under similar conditions. The simulations show how the model can both capture the general qualitative pattern of performance found in neuropsychological studies of search and make precise predictions open to empirical test.

To mimic unilateral PPC lesions, we reduced the number of neurons in the pools on one side of the location map. This would have the effect of reducing the signal from the affected brain region under structural imaging conditions. We report five simulations, three in Section 1 and two in Section 2. In Simulation 1, we examined whether a unilateral lesion would generate the qualitative pattern of selective disturbances in spatial and temporal search found in patients with PPC damage, where, compared with single-feature search, patients find both conjunction search and preview search abnormally difficult. We also assessed whether this selective difficulty was most pronounced for targets falling in the locations most affected by the lesion (e.g., the contralesional side of space in a patient). In Simulation 2, we investigated a particular variation of preview search used by Olivers and Humphreys (2004) in which the target and distractors appeared either within the same field or across different fields. This simulation served to distinguish predictions made by sSoTS from predictions made from an account that attributes impairments after PPC damage to problems in the spatial disengagement of attention (cf. Posner & Cohen, 1984). In Simulation 3 we report the results when, in addition to lesioning the model, we alter the general levels of activity through the model by lowering levels of excitatory neurotransmitter to mimic changes associated with lowered arousal (Posner & Petersen, 1990). Here we ask whether we find emergent deficits on the ipsi- as well as the contralesional side of space, consistent with nonspatial components of the neglect syndrome, as well as exaggerated deficits on the contralesional side. This last result would illustrate how a nonspatially selective factor (excitatory activity across the model) can interact with a spatially specific lesion to exacerbate problems in spatial selection. In Simulations 4 and 5 (Section 2) we more specifically evaluate sSoTS as a model for extinction, when selection of a stimulus on the contralesional side is disrupted by presentation of another item on the ipsilesional side. Simulation 4 assessed whether extinction was sensitive to the similarity between the stimuli in the ipsi- and contralesional fields. Simulation 5 examined how extinction varied as a function of the temporal relations between ipsi- and contralesional stimuli, assessing whether extinction varied according to whether the stimuli occurred simultaneously or successively. Di Pellegrino, Basso, and Frassinetti (1997; see also Baylis, Simon, Baylis, & Rorden, 2002) have shown that extinction is maximal when items occur simultaneously, presumably due to increased spatial competition for selection under these conditions. These simulations provide the first detailed modelling of temporal as well as spatial selection deficits in PPC patients, as well as the first computational exploration of nonspatial impairments in such cases.

In Section 3 of the paper we test predictions from the model that emerged from the simulations in Section 2. In particular, the data from Simulation 4 suggested that performance in the model was particularly sensitive to the similarity of the conjunctive relationship between ipsi- and contralesional stimuli under conditions of extinction. Also Simulation 5 predicted asymmetrical effects in selection over time, in which

performance was best when the contralesional item led in time. These predictions were examined in two patients, both of whom showed extinction to contralesional stimuli. The results show how computational models can go beyond serving as existence proofs (e.g., here for a parallel processing model simulating serial search) so that they are generative predictors of empirical data sets.

SECTION 1: SIMULATIONS OF GENERAL DATA SETS ON SEARCH AFTER PPC LESIONS

The architecture of the model

The model consists of spiking neurons organized into pools containing a number of units with similar biophysical properties and inputs. The simulations were based on a highly simplified case where there were six positions in the visual field, allowing up to six items in the final search displays.[1] sSoTS has three layers of retinotopically organized units, each containing neurons that are activated on the basis of a stimulus falling at the appropriate spatial position. There is one layer for each feature dimension ("colour" and "shape") and one layer for the location map (Figure 1). The feature maps encode information related to the features of the items presented in an experiment. The feature dimension "colour" encodes information on the basis of whether a blue or green colour is presented in the visual field at a given position i, ($i = 1, \ldots, 6$; creating activity in the blue and green feature maps). For simplicity, and given that many visual search experiments have utilized letter displays, we label the form maps as representing "letter shape" (there are two feature maps, one responding to the letter H and the other to the letter A). Note that we are not proposing that "letter maps" of this type exist in the brain, and all that is crucial for the present simulations is that one shape stimulus in the search task activates one map and the other a second map. The form maps here could equally well correspond to edge orientations (e.g., a map coding vertical edges would be differentially activated by H stimuli in the search task, and a map coding oblique edges would be differentially activated by A stimuli). The simulations were compared with data derived from the search tasks used by Watson and Humphreys (1997), which employed green H, blue H, and blue A stimuli, and thus for easy labelling we refer to "H" and "A" maps. The third layer contains the location map. The pools in the location map sum activity from the different feature maps to represent the overall activity for the corresponding positions in the visual field. Each of the layers contains one inhibitory pool (see also Deco & Rolls, 2005) and one nonspecific pool, along with the feature maps. The inhibitory pools are modelled following Dale's hypothesis, which states that a neuron is either excitatory or inhibitory in all of its connections with other cells; although this law is not absolute it provides useful classification of cell populations (Tuckwell, 1998). The nonspecific pool contains neurons that are not involved in the encoding of any information presented in the visual field, and it simulates the neurons that are present in the relevant brain area, but that are not involved in the studied processes. These neurons can have spontaneous activation and are connected with the corresponding feature maps for each layer. The ratio between inhibitory and excitatory neurons is the same for all the layers and is based on a ratio of 20−80, derived from populations of (inhibitory) interneurons and (excitatory) pyramidal neurons in the brain (Abeles, 1991; Rolls & Deco, 2002). The model also simulates signals that the feature and location maps receive from other brain areas. These signals can be characterized as noise and are simulated using a Poisson noise distribution. The system receives this signal as external spontaneous activity with a value of 3 Hz, consistent with activity values observed in the cerebellar cortex (Rolls & Treves, 1998; Wilson, O'Scalaidhe, & Goldman-Rakic, 1994).

[1] Simulations with increased numbers of units can take an extremely long time to run.

For each layer the inhibitory and nonspecific pools are connected with the pools in the feature maps. The neurons within each location pool in the feature map are mutually excitatory and have strong coupling; the neurons from different location pools within each map are also excitatory but have low coupling. The inhibitory process within each layer operates through the inhibitory pool of neurons. In addition, each pool in the location map is connected in an excitatory manner with the pools in the feature maps that represent the same position in the visual field. These excitatory connections feed back activity to enhance the competition at the feature level. The system used and the connections are illustrated in Figure 1. The connectivity between the units at different positions (pool of neurons) was homogeneous across space so that there was not (for instance) greater connectivity within relative to across the visual field.

Spiking characteristics

Spiking activity in the system can be described by a set of coupled differential equations that give the time evolution of each neuron as a function of the other neurons. The neurons use integrate-and-fire functions (Tuckwell, 1998), which can be represented by a circuitry with parallel capacitance and resistance. Each neuron fires when the subthreshold membrane potential reaches a threshold, and after the firing the membrane potential is reset to a fixed value.

The formulation of the integrate-and-fire neurons was taken from Deco and Rolls (2005) and Liu and Wang (2001). This contains a frequency adaptation mechanism based on Ca^{2+}-activated K^+ current I_{AHP}. Each neuron contains recurrent excitatory postsynaptic currents with two components: (a) a fast component that is mediated by AMPA-like dynamics, and (b) a slow component mediated by NMDA-like dynamics. The external neurons are modelled by AMPA-like connections. Inhibition is modelled using GABA-like dynamics. Details describing the characteristics of the neurons are given in Appendix A.

In order to investigate the system's behaviour efficiently a mean field approach was initially used, following Deco and Rolls (2005) and Brunel and Wang (2001). In this approach each pool of neurons is simulated as one unit, so that the system approximates the original system of individual spiking neurons (see Brunel & Wang, 2001). At the mean field level, the system has dynamics that can be directly derived from the spiking neuron model[2] but operation of the model at this level is less computationally expensive. Thus simulations at the mean field level can be used to define the limits on parameters in the system, which can then be explored more systematically at the level of spiking neurons, in order to more precisely model the relevant data. Descriptions of the mean field approach used here are given in Appendix B.

sSoTS uses similar parameters to those used previously to simulate search within spiking-level neural networks (Rolls & Deco, 2002) but places stress upon three parameters that were fit to simulate patterns of normal human visual search; these are the $[Ca^{2+}]$-activated K^+ current (used to capture the process of frequency adaptation), the top-down excitatory bias given to target features, and the top-down inhibitory bias against distractors.

Frequency adaptation

Adaptation of firing is known to be a common property of spiking neurons (Ahmed, Anderson, Douglas, Martin, & Whitteridge, 1998), whereby after firing there is a decrease in the probability of the neuron spiking again, down to some steady state. Spike frequency adaptation can be produced by several different ion channels, each one with its own characteristics. However, it is believed that during the first 300 ms of adaptation the main effect stems from a slow $[Ca^{2+}]$-activated K^+ current (Madison & Nicoll, 1984). This

[2] This property distinguishes mean field approximations from high-level connectionist simulations, which cannot be derived back to the operation of spiking-level neurons.

mechanism has been modelled by Liu and Wang (2001), and their formulation is employed here. The frequency adaptation function provides, "for free", a passive component to preview search based on the length of time that items have been in the field.

In the present simulation, the average firing rate of the neurons in each pool is calculated. The slow $[Ca^{2+}]$-activated K^+ current will affect more quickly the pools with higher firing frequency, since their increased firing leads to quicker increases in the intracellular levels of $[Ca^{2+}]$. Following this, the frequency of firing within these higher firing pools will decrease. In sSoTS the spike frequency adaptation mechanism takes the form of inhibition applied proportionately to the pools that are active for some period, where an active pool is one where the frequency of firing is relatively high compared with the other pools. An active pool in the feature maps indicates that there is an item in their corresponding position in the visual field.

Under conditions of preview search the I_{AHP}-current leads to a decrease in activation in pools that represent the positions of the first set of distractors, because these items are active for a period before the presentation of the search display.

Active inhibition

In psychophysical studies using probe dot detection it has been found that probes are difficult to detect if they fall at the locations of old distractors, compared to when they fall at the locations of new distractors or at previously unoccupied locations (Agter & Donk, 2005; Humphreys et al., 2004 Olivers & Humphreys, 2002; Watson & Humphreys, 2000). When participants receive the same displays but are not set to prioritize the new items for search, this bias against old locations disappears. This is consistent with participants inhibiting the locations of old items in the search task in order to prioritize attention to the new items. Olivers and Humphreys (2002) also found that this apparent suppression effect reduced if participants were given a secondary task at the time the initial distractors were presented as a preview, suggesting that any inhibition of old distractors is dependent on an active set (disrupted by a secondary task). Other data indicating active effects of distractor suppression in preview search come from studies of colour carry-over effects. Braithwaite and colleagues. (e.g., Braithwaite & Humphreys, 2003; Braithwaite, Humphreys, & Hulleman, 2005) have shown that, under preview conditions, RTs are slowed if the target carries the colour of the old distractors (compared to when it carries a different colour). This occurs even when the colour of the old items changes when the new search items are presented along with the target, indicating that the effect is not due to the new target grouping by colour with the old stimuli. The data are consistent with the features as well as the colours of the old items being inhibited and with the inhibition spreading to a new target with the same colour (see Duncan & Humphreys, 1989, for a discussion of spreading suppression). These data on target detection are matched by results on probe detection, if probes appear on new items sharing their colour with old stimuli (Braithwaite et al., 2005). This apparent inhibition effect is eliminated, however, if participants only perform the probe task and do not attempt to actively segment the old and new stimuli for search. Thus the effects are not due to the display conditions but due to the selection processes employed to optimize search.

The psychological argument for a role of active suppression of old stimuli is bolstered by our simulations with sSoTS, where we have found that, even with the $[Ca^{2+}]$ parameter optimized, search slopes found in human preview search are more easily approximated when active inhibition is incorporated into the model (Figure 2b). The efficiency with which humans ignore old items in preview search is matched when the active inhibition parameter is introduced into the model.

Top-down excitation

The third main parameter in our simulation was for top-down excitation of target features. The idea that search is guided by top-down excitation is

common to a number of current models of human visual search including, for example, guided search (Wolfe, 1994) and integrated competition (Duncan et al., 1997), and it is matched by psychological evidence demonstrating that search efficiency is aided when participants are given knowledge of the upcoming target in a display (e.g., Anderson, Heinke, & Humphreys, in press; Hodsoll & Humphreys, 2001). In the present simulations, a parameter was set for top-down activation of the pools corresponding to the target's features.

Parameter setting

The parameters for the simulations were established in baseline conditions in the unlesioned version of the model with "single-feature" and "conjunction" search tasks as reported by Watson and Humphreys (1997; conjunction search: blue H target vs. green H and blue A distractors; feature search: blue H target vs. blue A distractors). The generation of efficient and less efficient (linear) search functions in these conditions replicates the results of Deco and Zihl (2001). These same parameters were then used to simulate preview search. The parameter w^+ represents the strength of connections between the neurons in each pool, while w^- represents the strength of connections between the pools within and across each feature map. The target also benefited from an extra top-down input λ_{att} given to those feature maps that represent the target's characteristics (i.e., the colour blue and the letter H). The parameters for the $[Ca^{2+}]$-sensitive K^+ current were selected in order to be able to simulate the preview effect in addition to conjunction and single-feature search, when the model was unlesioned (search efficiency in the preview condition matching that in the single-feature baseline; Watson & Humphreys, 1997). Figure 2a shows the form of the function for the $[Ca^{2+}]$ parameter, and Figure 2b shows variation in the performance of sSoTS as the adaptation and active inhibition parameters are varied. The presence of an object in the visual field was signified by adding an additional λ_{in} value given to the external input that the system received. Overall the input that a pool could receive was (ext = (ext + ((in + (att)/Next. The parameters used for the system can be found in Deco and Rolls (2005). In preview search top-down attention ((att) was applied to the target's feature maps at the onset of the search display.

The parameters for the baseline search tasks were set using the mean field approximation, to simplify the search of the parameter space (see Mavritsaki et al., 2006, 2007, for fuller descriptions). Reaction times (RTs) were based on the time taken for the firing rate of the pool in the location map to cross a relative threshold (thr). If the selected pool corresponded to the target then the search was successful (a hit trial). If the pool that crossed the threshold corresponded to a distractor rather than the target then the target was "missed". Note, however, that if the parameters were set so that the target's pool was the winner on every trial, only small differences in the slopes were observed between conjunction and single-feature search, due to target activation saturating the system. Accordingly, search was run under conditions in which some errors occurred, mimicking human data. Only target present trials were simulated. Detailed simulations were run at the spiking level only (Watson & Humphreys, 1997; Watson et al., 2003). In simulations run at the spiking level there is noise within the system based on a Poisson distribution of activity in the units. This generates variance across different runs of the model and enables us to analyse the data by treating each run as a separate participant, matching studies with human participants . By analysing the data in this way we can test whether a given simulation holds across the population of possible runs of the model, within the parameters set. Also, due to the varying levels of noise, the model gives rise to predictions about the variance in responding as well as the mean level of responses, for example after brain lesions are introduced. This was tested here. One other attribute of spiking level simulations is RTs are generated using the real-time properties of the neurons, and thus search times in the model can be directly related to RTs generated

by human participants. The parameters used for the simulations are shown in Appendix C. Activity profiles for the single-feature and conjunction search conditions, in the unlesioned versions of the model, are provided in Figure 3. The model operates as follows. First, pools in the feature maps that represent characteristics of the targets are given extra excitation, relative to the features of distractors (here there is extra activation for the feature maps BLUE and H compared with the maps for the distractor features GREEN and A). In the single-feature condition (blue H target amongst blue A distractors—see Watson & Humphreys, 1997), the units in the H pool at the target position show a rapid rise in activation relative to units in the blue feature pool, due to the blue feature also representing distractors. This rapid rise in activation leads to strong excitatory feedback from the location map to the feature pool, and there is a subsequent iterative rise in activity enabling the target's location to be selected (activated above threshold level). In conjunction search there is a slower gain in activation in both the feature and location maps due to both of the target feature pools also being activated by the distractors (whereas only one feature pool is activated by distractors in the single-feature search condition). The increased competition in conjunction search leads to the target position winning the competition for selection much later in conjunction than single-feature search, while the peak activation in the location map is also

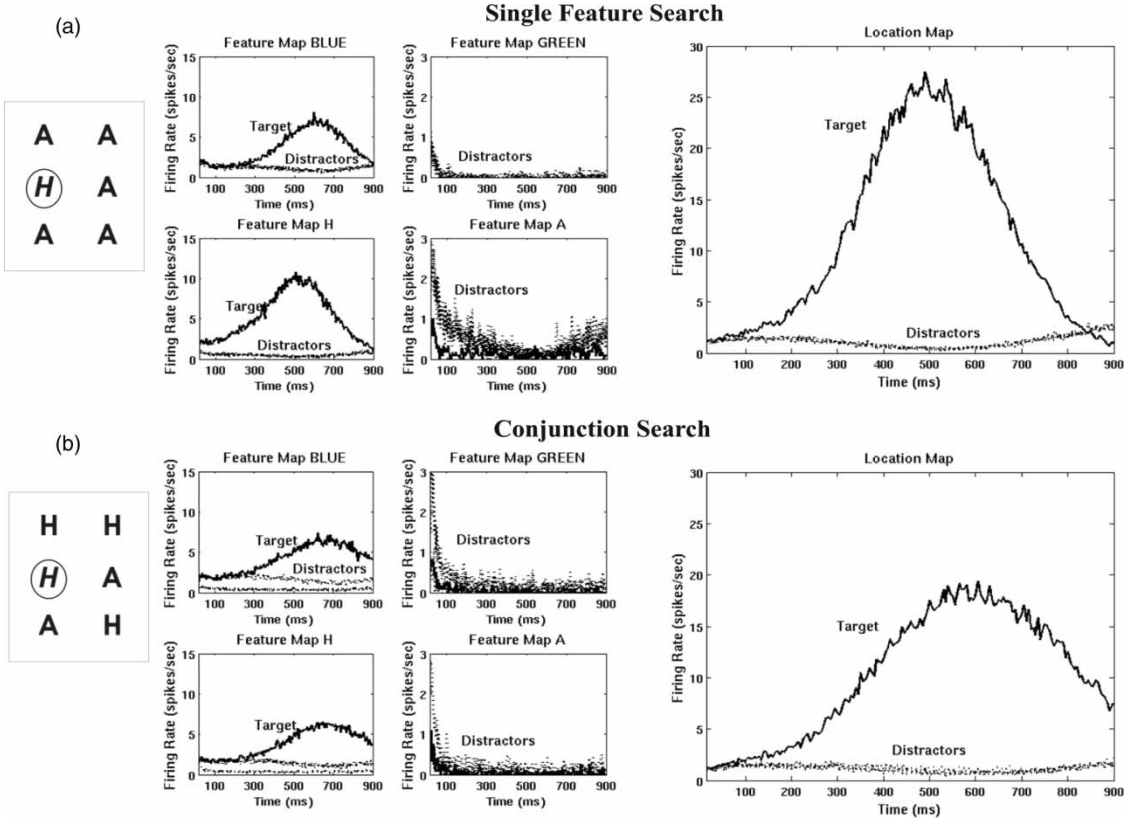

Figure 3. *Activation profile for units representing the location of the target in the feature and location maps in single-feature and conjunction search. Due to increased competition caused by targets and distractors sharing features and creating a less clear "winner" in the location map in conjunction search, detection of the target's location is delayed.*

reduced. Activity in the feature and location maps in the single-feature and conjunction conditions is shown in Figure 3. In the single-feature condition the amount of competition in the H map varies little as the number of distractors increases, and RTs to select the target change little too: There are efficient search functions. In contrast, the competition for selection in conjunction search increases as more distractors are added, slowing RTs. Inefficient search functions are generated, even though selection continues to operate in a spatially parallel manner. Figure 4 shows activation in the location units in the preview condition. Here there is initial activation for units occupied by distractors presented during the preview period, which decays through the operation of the $[Ca^{2+}]$ parameter. Due to this decay mechanism, plus also top-down inhibition applied to the features and locations of old distractors, these distractors do not compete strongly

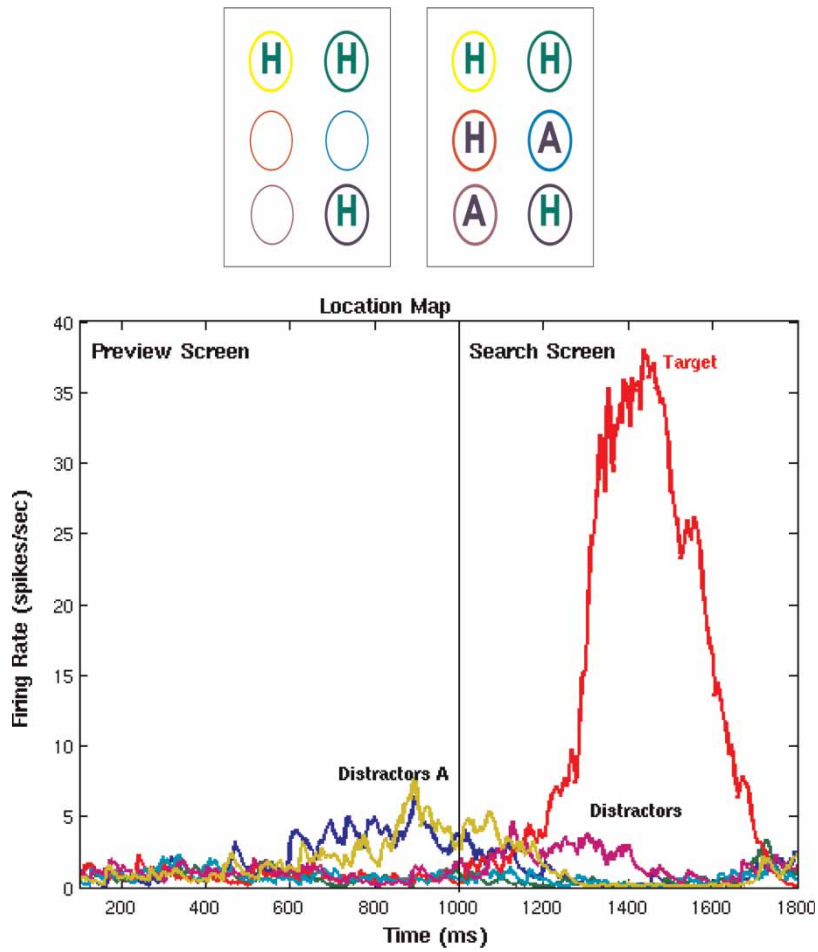

Figure 4. *Activation profile for units at the target's position in the location map in preview search. The display on the top left indicates which of the six field locations were occupied by a distractor during the preview period. The subsequent (right) display indicates which locations are occupied by old distractors and new search items, in the search display. The different colours represent contrasting locations. Due to competition between the distractors, frequency adaptation, and the additional active inhibition, the distractors do not respond strongly at the time of the new search display. To view a colour version of this figure, please see the online issue of the Journal.*

with the new items following presentation of the search display. As in the single-feature condition, the competition also does not rise greatly as additional distractors are added, so that search again is efficient.

To stabilize the system and to identify the parameters required to allow the model to approximate normal human search performance, the mean field approximation was used to identify. Here we explored the areas in parameter space in which the network converged to select the target when presented with input and areas in which convergence was not achieved (see Mavritsaki et al., 2006). We then used the parameters for which the network converged when presented with input to fix the parameters to generate patterns of single-feature and conjunction search matching those reported by Watson and Humphreys (1997). Finally, we explored the effects of the adaptation and active inhibition parameters (influential for preview search but not for search when all the items appear simultaneously) in order to simulate successfully the search slopes for preview search (Watson & Humphreys, 1997; see Figure 2b).

After setting the parameters for the unlesioned model, relative to data from normal human search, sSoTS was "lesioned" by reducing the number of units in the pools on one side of the location map (to approximate the effect of a unilateral parietal lesion). In the simulations of search (Simulations 1–3) we reduced each pool of location units by 16.66%. In the simulations of extinction, which may be thought of as a milder form of neglect (though see Karnath, Himmelbach, & Kuker, 2003), the pools of location units on the "contralesional side" were each reduced by 12.5%. In addition, in studies of extinction patients may only be asked to decide whether they detected a stimulus on the contralesional side, and they may not have to discriminate a target and distractors (cf. Gilchrist et al., 1996). To simulate this in sSoTS we ran the model without employing any top-down expectation for a particular target (e.g., a blue H). Here we examine the model's ability to discriminate the presence of a stimulus in the affected field purely using bottom-up cues.

SECTION 1: QUALITATIVE SIMULATIONS OF SEARCH AFTER PARIETAL DAMAGE

SIMULATION 1: EFFECTS OF A UNILATERAL LESION ON SEARCH THROUGH SPACE AND TIME

Eglin et al. (1989) and Riddoch and Humphreys (1987) reported that unilateral parietal lesions disrupt conjunction search more than single-feature search tasks. Humphreys et al. (2006) and Olivers and Humphreys (2004) also reported that unilateral parietal lesions impair preview search relative to feature search. In the first simulation we examined how a unilateral lesion influenced single-feature, conjunction, and preview search comparing the data qualitatively to those documented in the above studies.

Method

In all cases the target was a blue letter H. In the single-feature condition, the blue H appeared amongst a set of blue A distractors. In the conjunction condition, the blue H target appeared amongst a set of blue A distractors and green H distractors. In the preview condition, the green H distractors were presented first for 1,000 ms and remained in the field when the blue H target plus the blue A distractors were subsequently presented. These search stimuli then stayed in the field until the target was detected. These display conditions mirror those used by Watson and Humphreys (1997). Displays in the single-feature condition contained 2, 3, 4, or 6 items. Display sizes 2 and 3 corresponded to the final search display in the preview condition, while display sizes 4 and 6 corresponded to the number of items in the conjunction display. In the conjunction there were either 4 or 6 items in each display. In the preview there were either 2 or 3 distractors in the initial display, followed by the equivalent number of items in the search display (see Watson & Humphreys, 1997). The old items retained their locations in the field when the new stimuli appeared. In each case the stimuli were randomly

positioned in the field. Performance was averaged across the different permutations of the displays to create data equivalent to the results from 1 participant.

Results

To test the reliability of the results, sSoTS was run consecutively across all the display permutations in one condition to generate an average set of results for 1 "participant", and this was performed over 20 consecutive occasions (with different noise values) to simulate results for 20 participants. On half the trials the target was on the contralesional side (where location units were lesioned), and on half it was on the ipsilesional side (unlesioned location units). The data for the correct RTs for each "participant" were then entered into a within-subjects design analysis of variance (ANOVA), with data missing where there were no correct target detections in a given condition for 1 "participant". We compared each search condition against each other with the factors being lesion (unlesioned vs. lesioned version), search condition, display size, and target field. For the unlesioned model, the left and right side targets were randomly assigned to the contra- and ipsilesional fields for these analyses. Target misses were examined in similar ANOVAs with the average percentage of misses per "participant" (across the different display permutations) entered as the dependent variable.

Figure 5a gives the mean correct RTs in the unlesioned and lesioned versions of the model as a function of the target field and the display size, and Figure 5b presents the mean percentage of target misses. The data are plotted separately for comparisons of the preview condition against the single-feature and conjunction conditions (following Humphreys, Watson, & Jolicoeur, 2002). The number of items in the final preview search display matches the number of items in the single-feature search condition. If search is equally efficient in the conditions then the slopes of the search functions should not differ. The total number of items in preview search match those in the conjunction display. If preview search is more efficient than conjunction search, then the slope of its search function, based on the total number of items present, should be reduced. These different comparisons are mostly clearly shown by providing plots against the different display sizes. In the comparisons of the preview conditions with the single-feature and conjunction conditions, we used display sizes 2 and 3 from single-feature search and display sizes 4 and 6 from the conjunction search task. Comparisons between the single-feature and conjunction task were based on display sizes 4 and 6 in each case, so the number of items in the final displays were matched. Figure 6 gives the data for accuracy of report in the lesioned version of the model. Note that errors in the unlesioned version of the model were minimal and resembled those found to ipsilesional targets in the lesioned model.

Mean RTs

For the comparison between the single-feature and conjunction conditions there were significant main effects for each variable: search condition, target location, display size, and lesion, $F(1, 11) = 10.85$, 175.62, 5.80, and 6.65, respectively, all $p < .05$. RTs were slower for conjunction than for single-feature search, for contra- than for ipsilesional targets, for larger display sizes, and in the lesioned version of the model. There was one reliable interaction between target location and lesion, $F(1, 11) = 175.62$, $p < .001$. RTs were slower to contra- than to ipsilesional targets only after the lesion. The RT analyses for these comparisons are hampered by the relatively high error rate in the conjunction condition.

For the comparison between the single-feature and preview conditions there were reliable main effects of search condition, target location, display size, and lesion, $F(1, 19) = 1.97$, 430.0, 31.0, and 11.4, respectively. There was a reliable three-way interaction between the search condition, the target location, and the lesion, $F(1, 19) = 11.89$, $p < .01$. RTs were slowed in the preview condition relative to the single-feature condition, particularly for contralesional targets after the lesion.

The comparison between the conjunction and preview conditions revealed reliable main effects again of search condition, target location, display size, and lesion, $F(1, 13) = 10.35$, 155.74, 22.48,

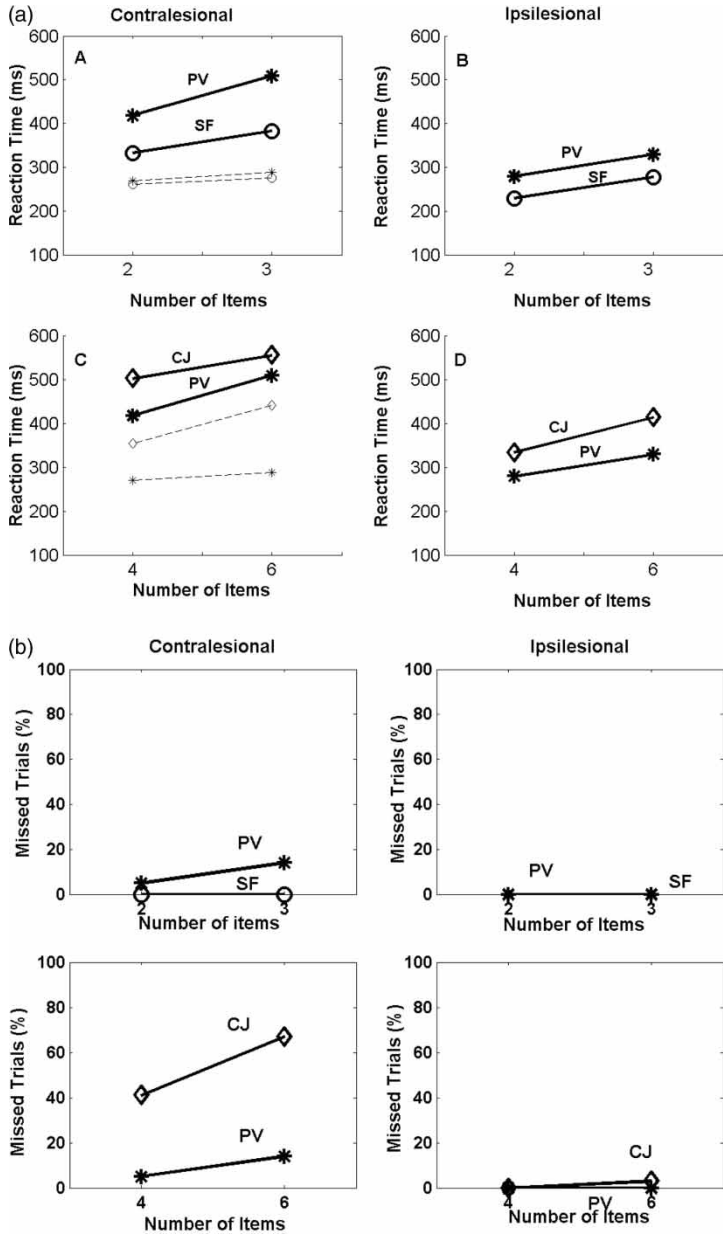

Figure 5. *(a) The mean correct reaction times (RTs, in ms) for the unlesioned (dotted lines) and lesioned versions (solid lines) of search over time and space (sSoTS). Data for the unlesioned model are plotted for convenience in the "contralesional" slide, but the data are for targets shown on either side of space. A illustrates the RT data for contralesional targets (in the lesioned model) for preview and single-feature search, plotted against the display sizes in the search display. B illustrates RT data for ipsilesional targets for preview compared with single-feature search. C shows the data for contralesional targets (in the lesioned model) plotted against the full display sizes for preview and conjunction search. D shows RT data for ipsilesional targets for the preview condition relative to the conjunction condition. The separate plots for preview search against the display sizes in the single-feature and conjunction search baselines follow the procedure used by Humphreys et al. (2002; data from Simulation 1). (b) Mirrors the RT data for the percentage of missed targets. SF: single feature; CJ: conjunction; PV preview. To see a colour version of this figure, please see online version of article.*

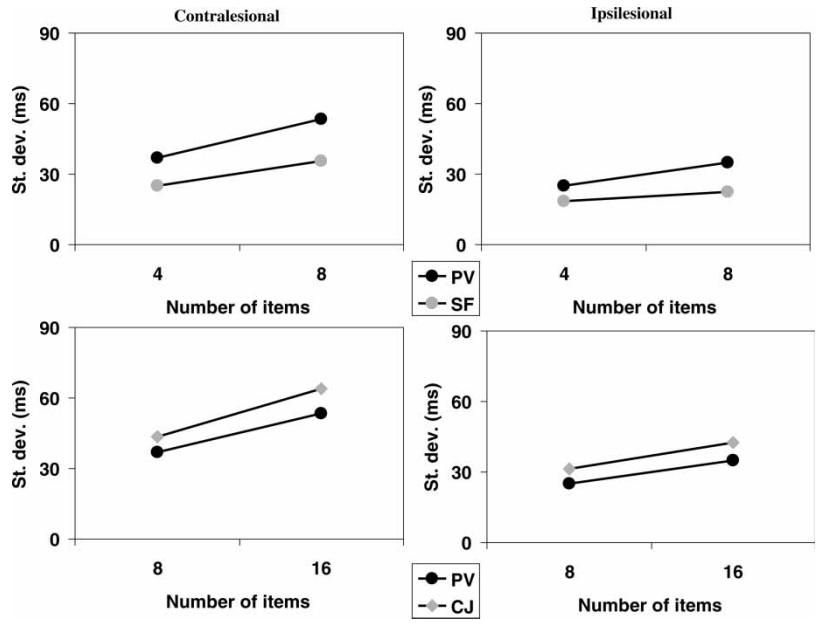

Figure 6. *The standard deviations in RTs shown by the lesioned version of search over time and space (sSoTS), run with different noise values, with contra- and ipsilesional targets. The top figures show performance as a function of the number of items in the single-feature display and the new search display for preview trials (for contralesional and ipsilesional targets). The bottom figures show performance as a function of the number of items in the conjunction display and the final display of both old and new items (for contralesional and ipsilesional targets. SF: single feature; CJ: conjunction; PV preview.*

and 4.61, all $p < .05$. There was one 2-way interaction between target location and lesion, $F(1, 13) = 55.7$, $p < .001$. The slowing of RTs to contralesional targets only occurred after lesioning. This did not differ reliably between the preview and conjunction conditions.

Accuracy

For the comparison between the single-feature and conjunction conditions there were reliable main effects of search condition, target location, display size, and lesioning, $F(1, 19) = 61.01$, 100.57, 12.24, and 50.16, respectively, all $p < .01$. There was also a significant four-way interaction, $F(1, 19) = 20.57$, $p < .001$. There were more errors in conjunction than single-feature search, but particularly for contralesional targets at the larger display size after lesioning.

The comparison between the single-feature and preview conditions revealed significant main effects, $F(1, 19) = 18.09$, 18.09, 4.54, and 18.09, all $p < .05$, for the effects of search condition, target location, display size, and lesioning. There was a four-way interaction between search condition, target location, display size, and lesion, $F(1, 19) = 4.54$, $p < .05$. The increase in errors in preview relative to single-feature search was most pronounced for contralesional targets at the larger display size after lesioning.

A comparison between the conjunction and preview conditions showed reliable main effects of search condition, target location, display size, and lesioning, $F(1, 19) = 55.69$, 235.79, 16.89, and 44.64, all $p < .001$. The four-way interaction was also reliable, $F(1, 19) = 3.88$, $p < .05$. There were overall more errors to contralesional targets at the larger display size after lesioning, with the effect being greatest in the conjunction condition.

Variance

The variance of search in neuropsychological patients for contra- and ipsilesional targets is

shown in Figure 7 (data taken from Humphreys et al., 2006). The equivalent data for the lesioned version of sSoTS are presented in Figure 6. The patients show a pattern in which there is increased variance per participant in the conjunction and preview conditions compared with the single-feature condition, and increased variance for targets falling in the contra- relative to the ipsilesional field. This same pattern is shown by sSoTS after lesioning.

Discussion

sSoTS was able to simulate normal patterns of search performance, when in an unlesioned state. First, conjunction search was slower and showed stronger effects of display size than the single-feature baseline condition. This provides an existence proof that a model with a parallel processing architecture can generate differences in search efficiency that match human data and that mimic serial search functions under more difficult discrimination conditions (see also Deco & Zihl, 2001; Humphreys & Müller, 1993, for earlier examples). Moreover, sSoTS also simulated human search over time, in the preview condition. The preview condition did not differ in search efficiency from the single-feature condition, while it was more efficient than the conjunction baseline (see also Mavritsaki et al., 2006, 2007). The preview benefit, relative to the conjunction condition, is brought about in the model both by the (passive) frequency adaptation process and by the (active) process of suppressing the old distractors. Note that, in all conditions, there was some effect of the display size. The display size effects even in the single-feature baseline match the data reported by Watson and Humphreys (1997) in a similar search task.

Of particular interest here are the results when sSoTS was "lesioned". The data demonstrate that lesioning led to costs that were most pronounced

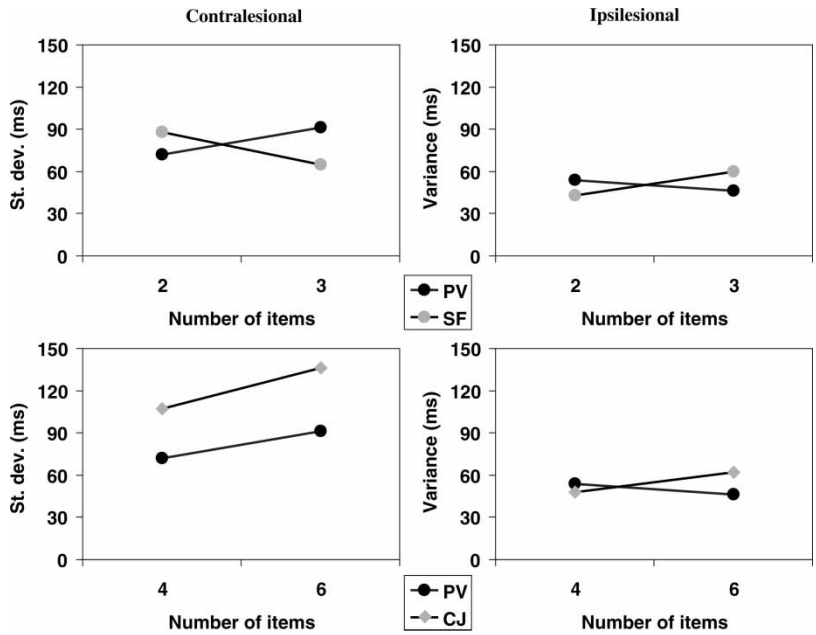

Figure 7. *The mean standard deviation in RTs, averaged across participants, for contra- and ipsilesional targets (taken from patients with posterior parietal lesions; Humphreys et al., 2006). The top figures shows performance as a function of the number of items in the single-feature display and the new search display for preview trials, for contralesional and ipsilesional targets. The bottom figure shows performance as a function of the number of items in the conjunction display and the final display of both old and new items, for contralesional and ipsilesional targets. SF: single feature; CJ: conjunction; PV preview.*

in the conjunction and the preview conditions. In terms of accuracy, the deficit was greater for the conjunction than the preview condition, and for both cases there were many misses of targets on the contralesional side. This was not due to a simple inability to process information on the contralesional side because similar costs were not apparent in the single-feature baseline. These failures to find the contralesional target arise due to the contralesional target being subject to strong competition, which meant either that a distractor was sometimes selected instead of the target or that there is no clear "winner" of the competition. Figure 8 shows activation functions in the location map for a target presented on the contralesional side of space with a display size of 4 for the single-feature and conjunction conditions (Figures 8a and 8b, respectively). The increased competition for selection is apparent, with there being a decreased difference in the activation functions for targets and distractors in the conjunction condition. The deficit for conjunction search is perhaps not surprising, given that conjunction targets have greater feature similarity with distractors than feature targets, and so should be subject to greater competition in any case (shown in the unlesioned model). When a conjunction target also appears on the contralesional side, then it generates less strong activation in the location map (there are fewer neurons to support a contralesional target)

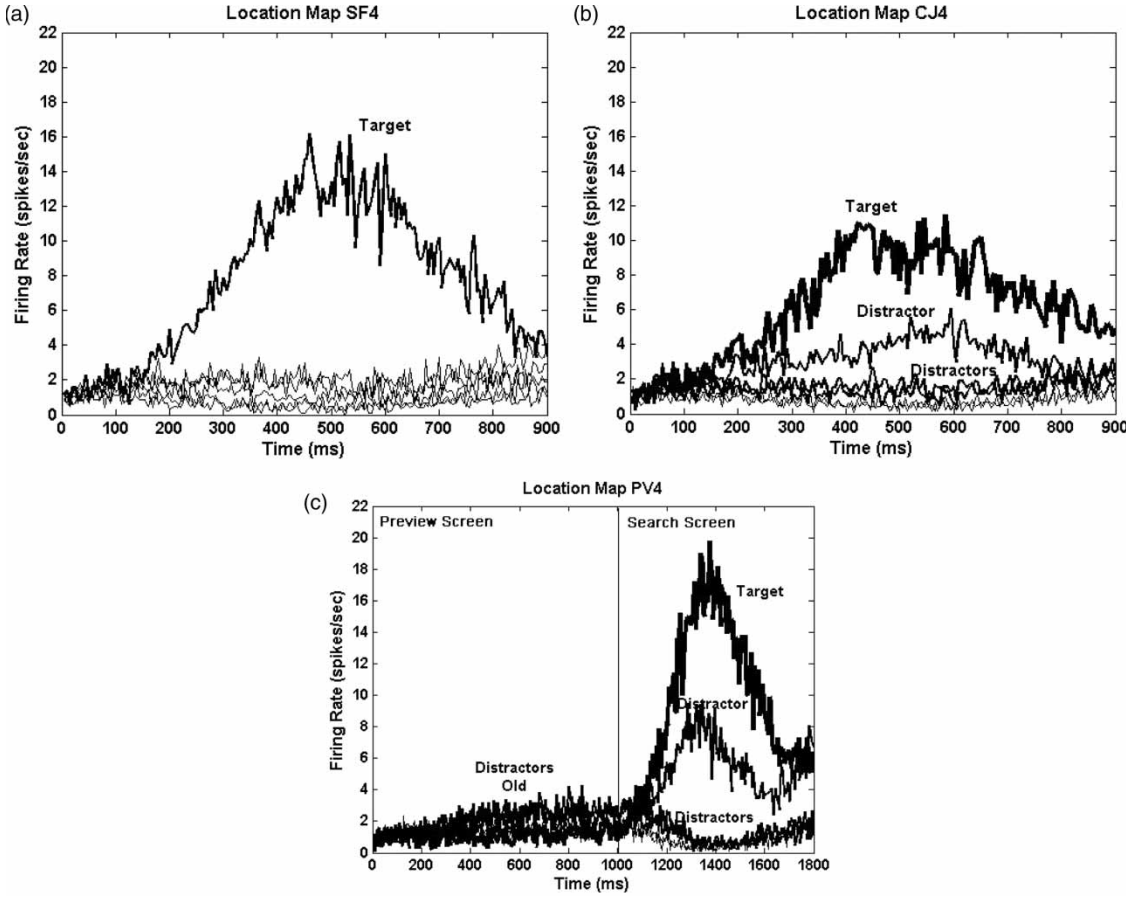

Figure 8. *Activation in the location map following lesioning, for contralesional targets at display size 4. (a) Single-feature (SF) search. (b) Conjunction (CJ) search. (c) Preview (PV) search.*

and less strong feedback to supporting units in the feature maps. In general terms, the target can be said to be less salient (cf. Itti & Koch, 2000). The emergence of weaker activity in undamaged feature maps is itself of some interest, since it matches functional imaging data in patients with PPC damage (Rees et al., 2000). The general finding that conjunction search is selectively disrupted, compared with a single-feature baseline, also replicates neuropsychological results (Eglin et al., 1989; Friedman-Hill et al., 1995; Riddoch & Humphreys, 1987).

The question arises, however, as to why the preview condition should also be more impaired by lesioning than the single-feature baseline. Note that neither of the critical mechanisms contributing to the preview benefit in the model—the frequency adaptation process and the top-down inhibition of old distractors—was directly subject to lesioning. However, although there is no direct effect of the lesion, the lesion does exert an indirect "knock on" effect, particularly on the frequency adaptation process. When lesioned, the activity for distractors on the contralesional side is reduced, so that consequently frequency adaptation can both be weaker and later-acting (when it takes place at all). This in turn means that old distractors can remain available to compete with new targets, making target selection more difficult. Figure 8c illustrates the increased competition after lesioning, with activation from a distractor increasing along with that for the target, once the search display appears. As contralesional targets suffer greater competition, these targets are most likely to be missed. This argument, about effects of lesioning on frequency adaptation is examined in more detail in Simulation 2. For now, we note that the result (with preview search being more disrupted than single-feature search) follows the pattern reported by Humphreys et al. (2006) and Olivers and Humphreys (2004) with PPC patients.

The accuracy data were largely replicated in the RT results. Both overall RTs and the slopes of the RT search functions tended to increase after lesioning, and effects were larger on conjunction and preview search than on the single-feature baseline. The one exception to this was conjunction search with contralesional targets, but the error rate in this condition was high, making it difficult to judge the RT data.

In addition to the effects on mean RTs and accuracy, there were also effects of lesioning on the variance of RTs. Following lesioning there was increased variance across different runs of the model, which was greatest for targets falling in the contralesional field. In addition, the variance was lower in the single-feature condition and increased in both preview and conjunction search, particularly for contralesional targets (Figure 6). Figure 7 presents the data from a group of parietal patients reported by Humphreys et al. (2006). As with the model, the patients showed increased variance for contralesional targets, and this effect was greater in the preview and conjunction conditions than in the single-feature condition. The increased variance in the model is a natural consequence of lesioning in a spiking level network, since noise is a function of the number of neurons present within the network (Noise $\sim\sqrt{}$/firing rate/number of neurons in the population). Reducing the number of neurons, by lesioning, will generate increased noise and more variance. The effects are greater in conditions where there is more noise from distractors (in conjunction and preview search after lesioning). These predictions, emerging naturally from the model, provide a good qualitative fit to the neuropsychological data,

SIMULATION 2: PREVIEW SEARCH WITH OLD AND NEW STIMULI IN THE SAME OR DIFFERENT FIELDS

Olivers and Humphreys (2004) reported one result that helps to throw light on the factors leading to impaired preview search in PPC patients. In their Experiment 3, they carried an orthogonal manipulation of whether the old and new search stimuli fell in the contra- and ipsilesional fields of the patients. One account for why preview search might be disrupted after PPC damage can be couched in terms of impaired disengagement of attention. Posner and Cohen (1984) originally

reported that patients with PPC lesions had difficulty in responding to contralesional targets particularly when their attention was cued to the ipsilesional side, and they argued that the patients had problems in disengaging attention from the ipsilesional side of space. Now, under preview conditions, there will typically be old distractors in the ipsilesional field. Consequently, patients may have difficulty in responding to new contralesional targets because they are impaired at disengaging attention from the old ipsilesional distractors. According to this disengagement account, preview search should be particularly difficult for PPC patients when the old distractors fall on the ipsilesional side and the new target on the contralesional side. Olivers and Humphreys (2004) did not find this, though. Instead they found that the patients were most impaired when the old and new stimuli fell in the same hemifield, irrespective of whether the target appeared on the ipsi- or contralesional side. The data argue against a spatial disengagement account of the deficit in preview search. Olivers and Humphreys (2004) put forward an alternative account, which was that PPC damage led to poor spatio-temporal segmentation of stimuli. As a consequence, performance of the patients was most impaired when their poor temporal segmentation (disrupting preview search) combined with conditions under which spatial segmentation was difficult (when the old and new items fell in the same hemifield). The precise mechanisms of spatio-temporal segmentation, however, were not specified. In Simulation 2 we evaluated whether sSoTS would give rise to a similar pattern of deficit to that observed by Olivers and Humphreys (2004) where presenting old and new items in the same hemifield was particularly disruptive to performance. In testing the effects of hemifield, we also assessed whether sSoTS could help us develop a more precise account of why spatio-temporal segmentation might be disrupted in the patients.

Method

The method was the same as that for Simulation 1, except that we orthogonally varied whether old and new items appeared in the contra- and ipsilesional hemifields for the model. Due to constraints on the number of items we could present in the displays, we were confined to using displays with just three items: one old distractor and one new distractor plus the target. As in Simulation 1, the target could appear on either the contra- or the ipsilesional side of space, but in each case it could appear either in the same field as the old distractor (the *within-field* condition) or in the opposite field (the *across-field* condition). Figure 9a gives example displays from the study. There were 20 permutations of the target and distractor locations in each condition, and these were presented four times in order to assemble the data for 1 "participant". Simulations were run to generate 20 participants. Only the preview condition was examined.

Results

The mean correct RTs (ms) and the percentage of correct trials are depicted in Figure 9b. The error rates were low in this experiment due to the small display sizes that were presented (see also Simulation 1, Figure 7). The error data were not analysed further.

The correct RTs were analysed in a repeated measures ANOVA with the factors being target field (contra- vs. ipsilesional) and display condition (within- vs. across-field). There was a borderline significant effect of the display condition, $F(1, 18) = 3.42$, $p = .08$, and of the target field, $F(1, 18) = 11.87$, $p < .01$. Furthermore, there was a significant Display Condition × Target Field interaction, $F(1, 18) = 7.34$, $p < .01$. The effect of target field (ipsi- vs. contralesional) was only reliable in the across-field condition, $t(18) = 4.78$. $p < .001$.

Discussion

These data simulate the results reported by Olivers and Humphreys (2004, Experiment 3). There were strong effects of whether old and new items appeared in the same or in opposite hemifields, and presenting targets in the same field as the old distractors was sufficient to overcome any advantage for the targets appearing on the ipsilesional

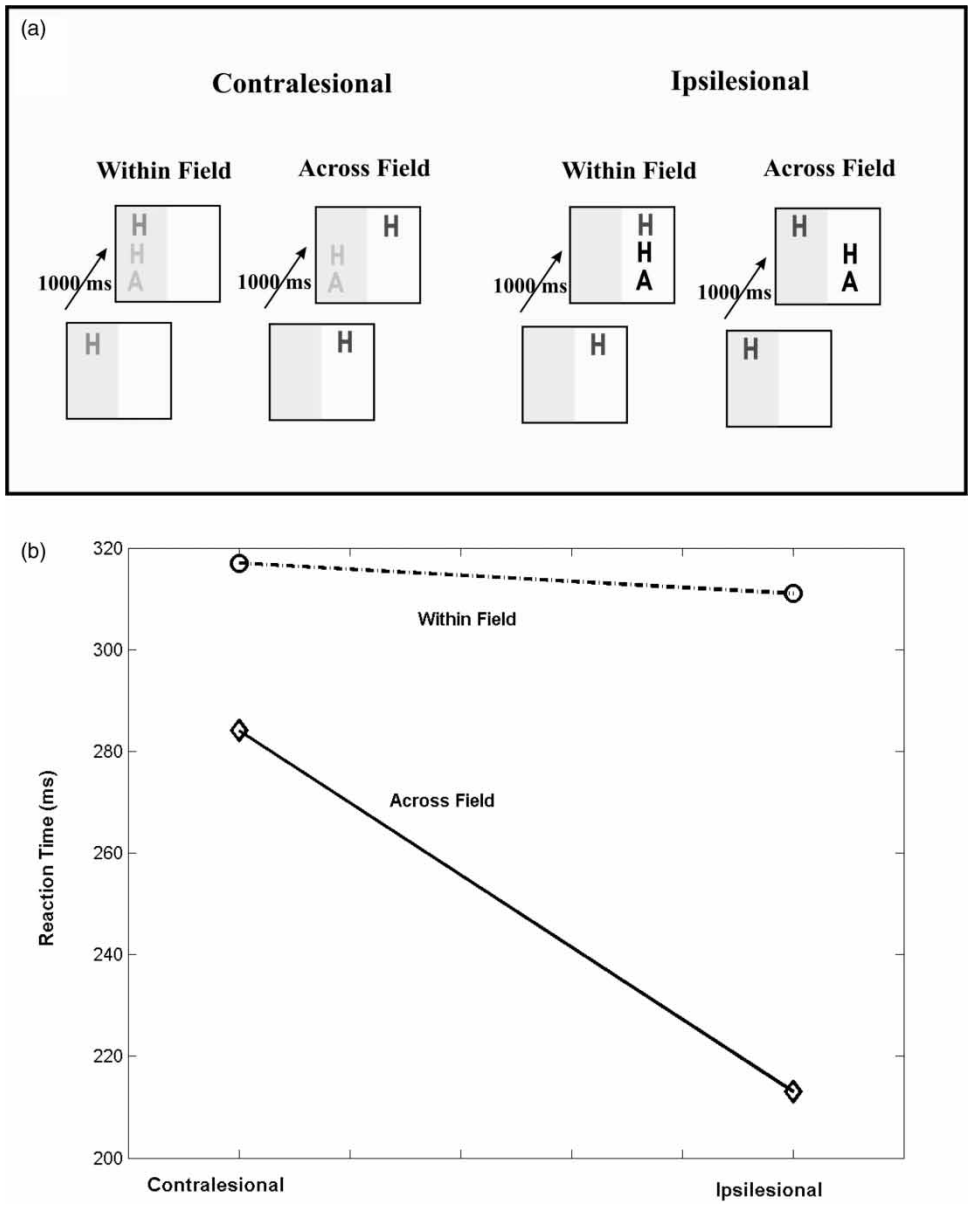

Figure 9. *(a) Example displays from Simulation 2. The shaded area of each display indicates the locations that were lesioned. (b) The mean correct reaction times (ms) from Simulation 2.*

side. Performance was easiest when the preview appeared in the contralesional field and the new targets in the ipsilesional field. As with Olivers and Humphreys (2004), the data contradict an attentional disengagement account of performance (cf. Posner & Cohen, 1984). According to the disengagement account, performance should be most difficult in the contralesional, across-field condition (when the old items appeared on the ipsilesional side, and the target fell in the contralesional field).

Rather than a disengagement account, sSoTS offers a different proposal. According to sSoTS the speed of search is determined by competition between the distractors and the target. The degree to which the old (previewed) distractor competes with the target is influenced by whether this distractor is suppressed at the time when the search display appears, along with the relative magnitude of activation for this distractor compared with the new target. An old distractor is less likely to be suppressed (by frequency adaptation), and any suppression will take longer to effect, when the item falls in the contralesional field. In addition to this, a contralesional item also generates reduced activity compared with an ipsilesional stimulus, and thus any accrual of activation in the location units also takes more time. These different factors can combine to generate the observed pattern of results. Search is easiest for an ipsilesional target following a contralesional preview (the ipsilesional, across-field condition) because the contralesional preview does not provide strong competition for selection, even if it is not suppressed at the time the search display appears, and activation accrues for the ipsilesional target. Search is most difficult for a contralesional target following a contralesional preview (the contralesional, within-field condition) because the target has relatively weak activation, and the distractor is not strongly suppressed at the time the target activation is accruing. Search for a contralesional target is better in the across-field condition because the ipsilesional preview is suppressed at the time that activation for the target accrues. This situation changes, however, with an ipsilesional target. In this case, a target can sometimes accrue activation before the ipsilesional distractor is suppressed, in which case the target suffers competition and slows selection. In conclusion, for sSoTS there is an interplay of influences that determine search efficiency based on the relative timing of suppression of the preview and of activation accrual and strength for the target. This interplay would be difficult to hypothesize without the explicit model.

SIMULATION 3: EFFECTS OF GLOBAL REDUCTIONS IN ACTIVATION

As we have noted in the introduction, patients with unilateral PPC lesions can show nonspatial as well as spatial deficits in visual selection. Furthermore, the presence of these nonspatial deficits may lie behind the more florid symptoms of neglect found in right- than in left-hemisphere lesioned patients, and they may led to the greater prevalence of neglect in right- than in left-hemisphere cases. Posner and Petersen (1990), for example, argue that the neural systems regulating arousal are lateralized within the right PPC, so damage to this region can produce problems in arousal than exacerbate any spatial bias in selection. This account links nonspatial selection problems to alterations in arousal in right-hemisphere cases (see also Robertson & Manly, 1999). In Simulation 3 we used sSoTS to provide an existence proof test of this proposal by globally reducing spontaneous activity within the model. We may assume that a similar global change in neuronal function could be caused by a right PPC lesion, in addition to the effect of the lesion on selection mediated by the location map. We ask whether this exacerbates the spatial deficit in the model.

Method

The method was the same as that in Simulation 1, except that we reduced global excitatory activation. This was done by decreasing NMDA-based activity throughout the model. Though this is not the neurophysiological mechanism for changing arousal proposed by Posner and Petersen (1990),[3] we believe it provides a first

[3] Posner and Petersen propose that arousal is modulated through the norepinephrine (NE) system. This system is not implemented within sSoTS, and to introduce it would mean changes to the operation of the basic model to accommodate a new neurotransmitter system. The effect of reducing NE is to globally lower activation levels. Our approach was to approximate this by decreasing NMDA activity, which has a similar global effect.

approximation to the effect and enables us to modulate activation levels globally through the system. The question then is whether effects of spatial bias are increased through this global parameter change. Performance was tested under conditions of single-feature, conjunction, and preview search.

Results

The mean correct RTs (ms) and the percentage of miss responses are presented in Figure 10. Note that there were no correct detections of a contralesional target at display size 6 in the conjunction condition; hence data were averaged across the display sizes for the RT analyses.

RTs

Data were collected for the equivalent of 20 "participants" and were subjected to within-subjects ANOVAs. Performance was compared with that in Experiment 1, which simulated the effects of lesioning without changes in global excitatory activity. For the comparison between the single-feature and conjunction conditions the factors were: simulation (Simulation 1 vs. Simulation 3), search condition (preview vs. single feature), and target field (contra- vs. ipsilesional). The effects of simulation and target field were reliable, $F(1, 14) = 18.34$ and 164.36, both $p < .001$. RTs were longer in Simulation 3 than in Simulation 1, and they were slower for contralesional than for ipsilesional targets. There were no interactions.

In a similar comparison between the single-feature and preview conditions all the main effects were reliable, $F(1, 16) = 41.86$, 61.14, and 36.63, all $p < .001$. The three-way interaction was also significant, $F(1, 16) = 15.26$, $p < .01$. RTs were longer in Simulation 3 than in Simulation 1, they were longer in the preview than in the single-feature condition, and they were longer for contralesional targets than for ipsilesional targets. However, the increase in RTs was greatest for contralesional targets in the preview condition, when global activation was lowered (in Simulation 3). Nevertheless, taking just the ipsilesional target there was a reliable interaction between simulation and search condition, $F(1, 18) = 11.12$, $p < .01$. The increase in RT in Simulation 3 was greater in the preview condition.

The analyses comparing conjunction and preview search revealed main effects of simulation, search condition, and target field, $F(1, 14) = 69.31$, 7.36, and 53.51, all $p < .025$. The three-way interaction was again reliable, $F(1, 14) = 12.79$, $p < .01$. RTs were slowed in Simulation 3 compared with Simulation 1, they were slower in conjunction than in preview search and for contralesional targets. The difference between the search conditions was largest for contralesional targets in Simulation 3. Nevertheless, for ipsilesional targets alone there was a borderline interaction between simulation and search condition, $F(1, 14) = 4.20$, $p = .06$. The increase in RTs when NMDA was lowered (in Simulation 3) was greater in the conjunction condition.

Accuracy

The accuracy data were analysed in the same way. For the comparisons between the single-feature and conjunction conditions, there were reliable main effects of simulation, search condition, and target field, $F(1, 19) = 44.60$, 31.10, and 155.43, all $p < .001$. The interactions between search condition and target field and between simulation and target field were both significant, $F(1, 19) = 23.56$ and 37.27, respectively. Target misses were greater in Simulation 3 than in Simulation 1; they were increased in the conjunction compared with the single-feature condition and for contralesional targets. The effect of target location was greater for conjunction than for single-feature search, and it was greater when activation levels were globally reduced (in Simulation 3). Also, reducing global activity (in Simulation 3) increased the error rate even for ipsilesional targets considered alone, $F(1, 19) = 8.87$, $p < .01$.

The comparison between the single-feature and preview conditions revealed an overall main effect of simulation: higher errors in Simulation 3, $F(1, 19) = 12.01$, $p < .01$.

The comparison between the conjunction and preview conditions demonstrated significant main

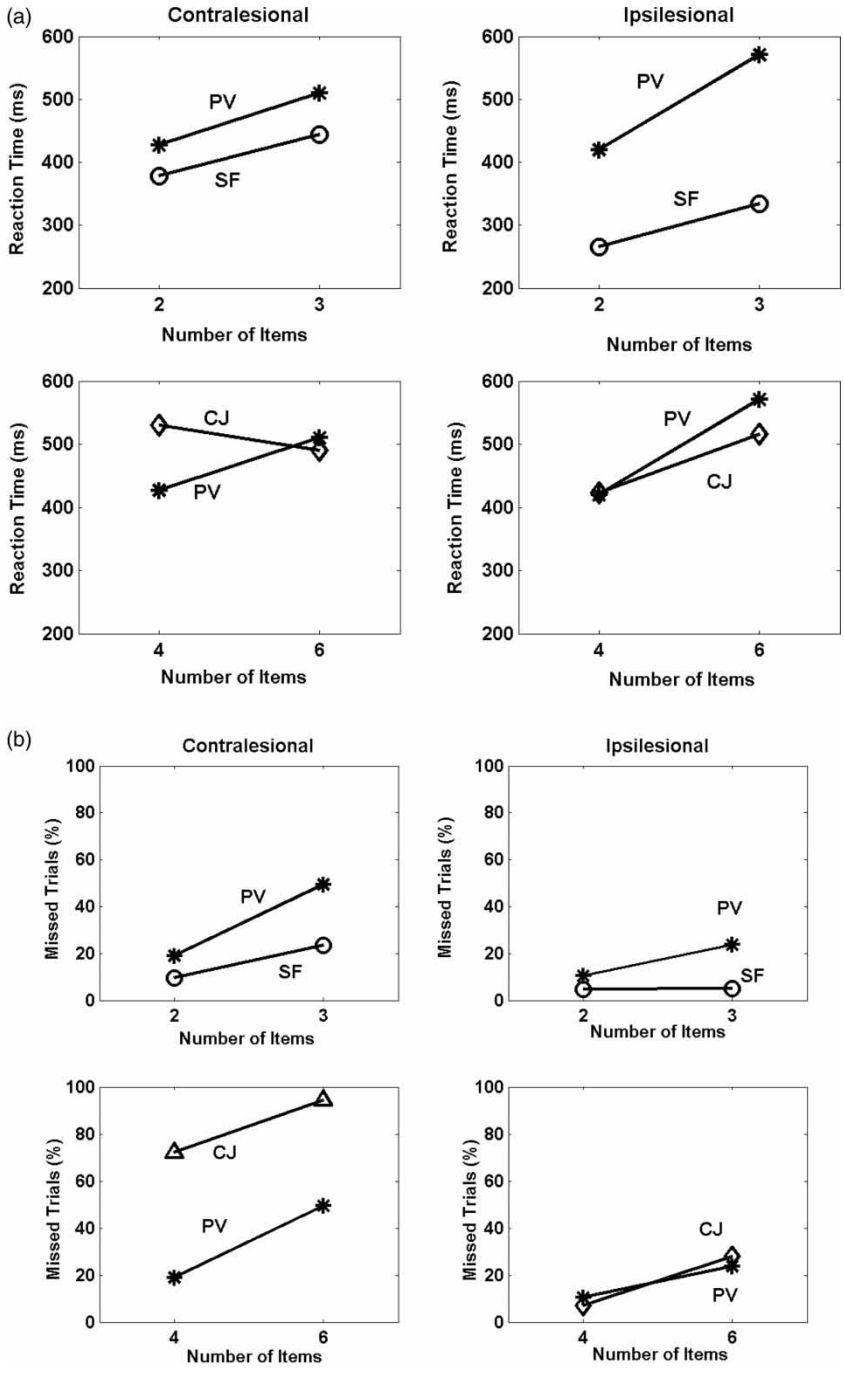

Figure 10. *(a) The mean correct reaction times (ms) and (b) the mean % miss responses for Simulation 3 (variation in global activation). The top figures illustrate performance with single-feature and preview displays, set against the number of items in the search display. The bottom figures present the results for the preview and conjunction conditions shown against the total number of items in the combined displays of the preview condition. Contralesional targets left; ipsilesional targets right. SF: single feature; CJ: conjunction; PV preview.*

effects of simulation, search condition, and target field, $F(1, 19) = 42.08$, 81.96, and 118.76, respectively. The three-way interaction was also reliable, $F(1, 19) = 7.91$, $p < .025$. There were more errors in Simulation 3 than in Simulation 1, more in the conjunction than in the preview condition, and more with contralesional targets. Taking ipsilesional targets alone, errors were still higher in Simulation 3 than in Simulation 1, $F(1, 19) = 4.14$, $p < .05$.

Discussion

The results show that performance generally decreased when global activation levels were lowered (in Simulation 3), while spatial biases in selection were exacerbated, compared with when there was only a unilateral lesion to the location map (Simulation 1). This greater impairment was most evident in the conjunction condition in accuracy, though RT costs were also selectively apparent in preview search compared with the single-feature baseline. Under conditions of a global reduction in activation, there was increased competition between targets and distractors, and this was most detrimental to search where the competition is greatest (e.g., in conjunction and preview search).

One other interesting aspect of performance was that problems increased for ipsi- as well as for contralesional targets, when excitatory modulation decreased (in Simulation 3). This provides evidence for a nonspatial deficit in selection, additional to any effects of the spatially selective lesion on selection through the location map. As we noted in the introduction, there is neuropsychological evidence for altered neurotransmitter modulation in patients showing unilateral neglect, which can be improved by appropriate drug treatment (Malhotra et al., 2005). Simulation 3 illustrates how reduced neurotransmitter modulation, to produce a global change in neural activation, can impact on the mechanisms of visual selection. The results provide a qualitative fit to neuropsychological data on the relation between neglect and arousal. Our data indicate that effects of spatial bias and global arousal do not just combine additively but interact to exacerbate spatial deficits in attention.

SECTION 2: MAKING PREDICTIONS ABOUT EXTINCTION

SIMULATION 4: EFFECTS OF GROUPING ON EXTINCTION

Simulations 1–3 examined effects of a relatively extensive lesion (removing 16.66% of the units in the pools of units on one side of the location map) on search of displays shown for unlimited presentation conditions. In Simulations 4 and 5 we assessed whether a pattern of extinction could also be observed when a smaller lesion was introduced (removing 12.5% of the units on one side of the location map) and when there was no top-down bias for a particular target (the task was to detect for any reliable activation on the contralesional side, in the location map). Without a top-down bias, we measure the ability to detect the target (due to corresponding location units being activated) rather than target identification.

In addition to testing for an extinction effect, we also examined the effects of additional variables, to generate novel predictions from the model. In Simulation 4 we assessed whether there were effects of grouping between the items on the magnitude of extinction. In this study, the displays contained either a single blue H (the target) or the blue H target along with a distractor that was (a) the same (a blue H), (b) different in shape but not colour (a blue A), (c) different in colour but not shape (green H), or (d) different in both shape and colour (green A). The target was always presented on the contralesional side, and we assessed detection of this contralesional item as a function of its relationship to the ipsilesional stimulus. In Simulation 5 we tested the effects of the temporal relationship between the ipsi- and contralesional stimuli. The specific effects of visual similarity and interstimulus timing, which arise as novel predictions from the model, were tested in Section 3.

Method

As noted above, displays always contained a contralesional target, which could appear alone or be accompanied by a distractor that shared 2, 1, or

0 features with it. The displays were exposed for 500 ms to mimic the reduced exposures typically used to elicit extinction in patients. The simulations were conducted for "20 participants".

Results

The results are presented in Figure 11. Data are depicted here averaged across the two 1-feature-shared conditions (the results did not differ according to whether the colour or the shape of the contra- and ipsilesional stimuli were shared).

Accuracy varied across the presentation conditions, $F(3, 57) = 11.86$, $p < .001$. Detection of a single target tended to be better than detection when there were two identical stimuli, $t(19) = 2.04$, $p = .06$. Detection of the target when it was paired with an identical stimulus was better than when it was paired with a distractor with one feature in common, $t(19) = 2.33$, $p < .05$, and performance in the last case did not differ from when the target appeared with a completely different distractor ($t < 1.0$).

Discussion

Simulation 4 shows that a pattern of extinction can be generated when sSoTS is spatially lesioned, and there is no top-down set to detect a particular target. Under these conditions there was relatively good detection of a single target presented on the contralesional side along with poor detection when

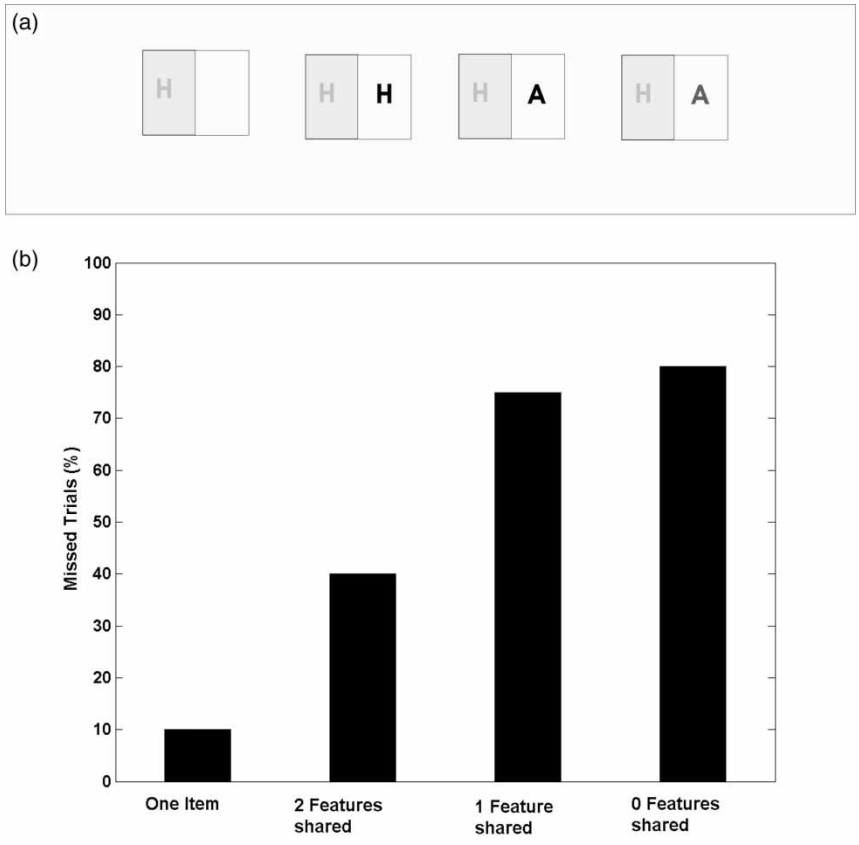

Figure 11. *(a) Example displays from Simulation 4 (effects of grouping on extinction). Shading indicates lesioned location. (b) The mean % miss responses in Simulation 4.*

the same item appeared for the same duration along with a completely different distractor. In addition to this, there was evidence that extinction was influenced by the similarity of the items. Extinction was reduced when the contralesional item was identical to an ipsilesional distractor,[4] compared to when there was only one feature shared with the target and relative to when there were no features shared between the target and the distractor. There was also a small trend for target detection to improve when the distractor had one compared with no features in common, and this difference was reliable for RTs. Positive effects of similarity on extinction have previously been reported when stimuli are similar in terms of shape and contrast polarity (Gilchrist et al., 1996; Humphreys, 1998), when their edges are collinear (Gilchrist et al., 1996; Mattingley et al., 1997) and when the stimuli together form a familiar shape (Kumada & Humphreys, 2001; Ward et al., 1994). Usually such results have been interpreted as reflecting grouping between the items, which enables the contralesional stimulus to be recovered as part of a perceptual unit along with the ipsilesional stimulus. However, sSoTS does not employ a mechanism for grouping, so how can these positive similarity effects come about? We suggest that the effects reflect the degree of within-dimension competition between the distractor and the target. When the stimuli are identical, there is no competition between the features within each feature dimension (though there remains competition, for example, introduced by feedback from the location units, which may still lead to some extinction compared to when the target appears alone). When the stimuli share only one feature there is competition within the nonshared feature dimension (e.g., between blue and green, if the stimuli are both Hs), and when they share no features there is competition within both feature dimensions, decreasing target detection. Note that the inhibitory weights for the model were set to mimic feature and conjunction search and not patterns of extinction, and it may be possible to tune the weights to lead to a difference between the one- and no-shared feature conditions, but the important point is that, even with the original weight parameters, positive effects of similarity were found. In Experiment 1 in Section 3 we test the prediction from sSoTS that there should be a differential reduction in extinction for identical stimuli over stimuli sharing one or no features.

The present pattern of results, where extinction reduced when the stimuli shared features, is also different from a pattern reported by Baylis, Driver and Rafal (1993; see also Baylis, Gore, Rodriguez, & Shisler, 2001). These investigators found that patients can show greater extinction when two stimuli had identical features along a response dimension than when the stimuli have different features. The results have been interpreted in terms of poor "token formation" in the patients caused by poor location coding on the contralesional side. Token representation may be needed in order to enter stimuli into visual short-term memory (VSTM). Due to having a degraded token representation, the patients should find it difficult to realize that a contralesional item has been presented when it is identical to the ipsilesional item. Interestingly, in studies reporting positive effects of grouping, patients have typically been asked to report only the presence of stimuli but in studies reporting negative effects of similarity the tasks have required the report of the location and identity of the stimuli. In addition, the stimuli have been presented at proximal locations in studies showing positive effects of grouping, whereas studies reporting negative effects of similarity have used widely spaced stimuli (e.g., 12° from fixation in Baylis et al., 1993). Performance is more likely to depend on individual token representations in VSTM when the items are widely spaced apart and coded separately into memory. The representation of stimuli in VSTM is beyond the scope of

[4] Note that this was not because the ipsilesional distractor was detected. Performance here was measured according to whether units at the target's position were activated above threshold in the location map.

the current implementation of sSoTS, and so data stressing token identification are not simulated here.[5] Instead of this, sSoTS can be thought of as simulating early stages of selection in which the presence of target is merely registered. It follows that sSoTS predicts that there should be positive effects of similarity in a target detection task, at least when the items are reasonably closely spaced, and any effects of similarity should increase when the stimuli have two rather than one feature in common. This was tested in Experiment 1 in Section 3.

SIMULATION 5: EFFECTS OF TEMPORAL RELATIONS ON EXTINCTION

Having established a basic extinction effect in Simulation 4, in Simulation 5 we examined the effects of the temporal relations between the stimuli on the extinction effect. Di Pellegrino et al. (1997; see also Baylis et al., 2002) reported that extinction was maximal when the ipsi- and contralesional stimuli appeared together, and it reduced when the stimuli were temporally separated. This is interesting because, like Olivers and Humphreys (2004, Simulation 2), the result again goes against an account in terms of impaired disengagement of attention. According to the disengagement proposal, the contralesional item should be particularly difficult to select when the ipsilesional item leads, since then there should be maximal initial engagement of attention on the ipsilesional side. We assessed whether the temporal dynamics of sSoTS would give rise to a pattern of performance similar to humans and stimuli are temporarily segmented.

Method

For these simulations we always used a blue H target and a green A distractor. The target always appeared on the contralesional side and the distractor on the ipsilesional side. Each stimulus was presented for 500 ms, and in the successive presentation conditions the offset of the first stimulus coincided with the onset of the second stimulus. There were three presentation conditions: contralesional item first; simultaneous items; ipsilesional item first. We assessed the proportion of trials where the location unit corresponding to the target exceeded its threshold. As before we ran 20 instances of the model with the noise varying across different runs.

Results

The mean percentages of report in the three presentation conditions are given in Figure 12. There was an overall difference across the three conditions, $F(3, 28) = 9.77$, $p < .001$. Accuracy was highest when the contralesional item led, $t(19) = 4.95$ and 2.99, $p < .01$, for comparisons with the simultaneous and ipsilesional first conditions. Accuracy was lowest when the stimuli appeared simultaneously, but the difference relative to the ipsilesional first condition was not reliable, $t(19) = 1.42$, $p > .05$.

Discussion

The general pattern of the data replicate those reported by Di Pellegrino et al. (1997) and Baylis et al. (2002). Extinction was maximized when the stimuli appeared simultaneously relative to when they appeared successively. This result occurs in sSoTS because competition is maximized when the stimuli appear together. When the contralesional item leads, there can be sufficient time for activation to accrue for this item to then withstand competition from the ipsilesional stimulus. When the ipsilesional item leads, the relatively fast identification of this item enables frequency adaptation to take place so that it again is a less strong competitor against the contralesional

[5] It should also be pointed out that negative effects of similarity have not been universally found even in experiments that use localization tasks (e.g., Kitadono & Humphreys, 2007, failed to find the effect across seven experiments in patients showing extinction).

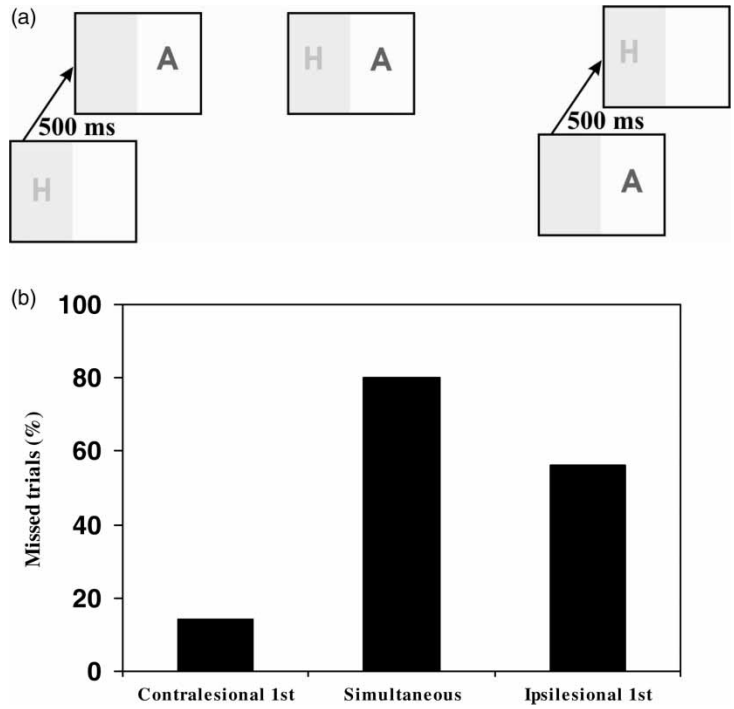

Figure 12. *(a) Example displays from Simulation 5 (effects of the temporal relation between items on extinction). Shading indicates lesioned location. (b) The mean % misses in Simulation 5.*

target. The results also indicate that, across the two consecutive presentation conditions, performance was better when the contralesional item led. This result goes against some of the findings in the literature on the effects of temporal intervals on extinction. For example, Di Pellegrino, Basso, and Frassinetti (1998) reported that longer intervals were required between the stimuli for both items to be identified when the contralesional item led than when the ipsilesional item led (see also Baylis et al., 2002). However, in these studies patients were required to identify the items, and the longer lag needed when the contralesional item led may be caused by slowed higher level identification of this stimulus compared with the ipsilesional item. If the identification of the contralesional item is slowed, the ipsilesional stimulus may offset before attention can switch to it. Under conditions where stimuli must only be detected, as simulated by sSoTS, the same result may not apply. For sSoTS, performance is best when the contralesional stimulus leads because the contralesional location then has least competition. Whether this prediction holds for PPC patients was examined in Experiment 2 in Section 3.

SUMMARY OF SIMULATIONS (SECTIONS 1 AND 2)

The simulations show that sSoTS, when lesioned, is able to capture patterns of results observed in human patients with PPC damage. There is selective impairment for conjunction and for preview search compared with single-feature search, and there are differential increases in the variance in conjunction and preview search after lesioning (Simulation 1). The deficit for preview search is affected by whether the old and new stimuli appear in the same or in opposite visual fields (Simulation 2). The spatially selective deficits in

the model worsen further when general levels of excitation are decreased by globally reducing excitatory activation, and this also leads to problems in selection on the ipsilesional side of space (Simulation 3). This mirrors data linked to decreased arousal in patients with right PPC lesions. The lesioned version of sSoTS can also be subject to extinction when there is no top-down set to detect a particular target, though extinction is offset to some degree by feature similarity between the contra- and ipsilesional stimuli (Simulation 4). Finally, sSoTS mimics some aspects of human data on the effects of the temporal relations between stimuli on extinction (Simulation 5). These results provide an existence proof that a model with the proposed architecture and dynamic processing characteristics can simulate several aspects of human performance. The model also presented some predictions about the effects of similarity and of stimulus timing on extinction—namely, that patients can be sensitive to conjunctive relations between the contra- and ipsilesional stimuli (Simulation 4), and the performance with successively presented stimuli can be better when the contralesional item leads than when it follows. These predictions were subsequently tested in Section 3.

SECTION 3: EXPERIMENTAL TEST OF THE PREDICTIONS FROM SECTION 2

EXPERIMENT 1: EFFECTS OF SIMILARITY ON EXTINCTION

Experiment 1 examined the effects of similarity on extinction. The task involved patients deciding whether 0, 1, or 2 stimuli had been presented in the visual field. The stimuli were the letters O and E, which could be coloured red or green. There were equal numbers of single-item trials with each Letter × Colour combination. There were four types of two-item trial: (a) identical conjunctions (e.g., two red Os); (b) letters sharing their colour but not their identity (red O, red E); (c) letters sharing their identity but not their colour (red O, green O), and (d) letters differing in both colour and identity (red O, green E).

Method

The experiment was conducted with two patients with unilateral right-hemisphere lesions involving the inferior parietal, superior temporal, and inferior frontal lobes, T.M. and M.P. Figure 13 presents a transcription of their MRI scans (3T T1 structural at 1 mm isotropic resolution). M.P. was 58 years old at the time of testing. He was a left-handed, former toolworker who had suffered an aneurysm 13 years previously. He had problems in mathematical abilities (see Humphreys, Watelet, & Riddoch, 2006c) along with aspects of visual neglect. On line crossing from the Behavioural Inattention Test (BIT; Wilson, Cockburn, & Halligan, 1987), M.P. scored 28/36, missing items in the final left column; in the star cancellation task he omitted all of the target stars on the far left and cancelled 9/19 stars in the next left column. In a line bisection task with lines placed randomly on a page, he omitted all items on the left and showed an average shift of 3% toward the right; he identified the gender of the left side of male–female chimeric faces on just 5/20 trials responding in all other trials to the gender of the right-side face (see Forti & Humphreys, 2005).

T.M. was 75 years old at the time of testing and was a former publican. He too showed evidence of neglect. In the star cancellation task (Wilson et al., 1987) he missed the last 5 stars on the left, near quadrant, and he missed 4 lines in the left near quadrant on the line crossing task. Given male–female chimeric faces he identified the gender of 13/20 of the left- as well as the right-side face, but on seven trials he just reported the gender of the right face. Both patients showed evidence of left extinction when presented with two-item displays for duration similar to those used in the simulations with sSoTS (T.M., 350 ms; M.P., 500 ms).

Both patients received 226 trials, presented in two sessions. There were 24 trials in each of the 4 two-item conditions, 96 single-item trials (48 left, 48 right), and 24 zero-item trials. The task was to decide whether there were 0, 1, or 2

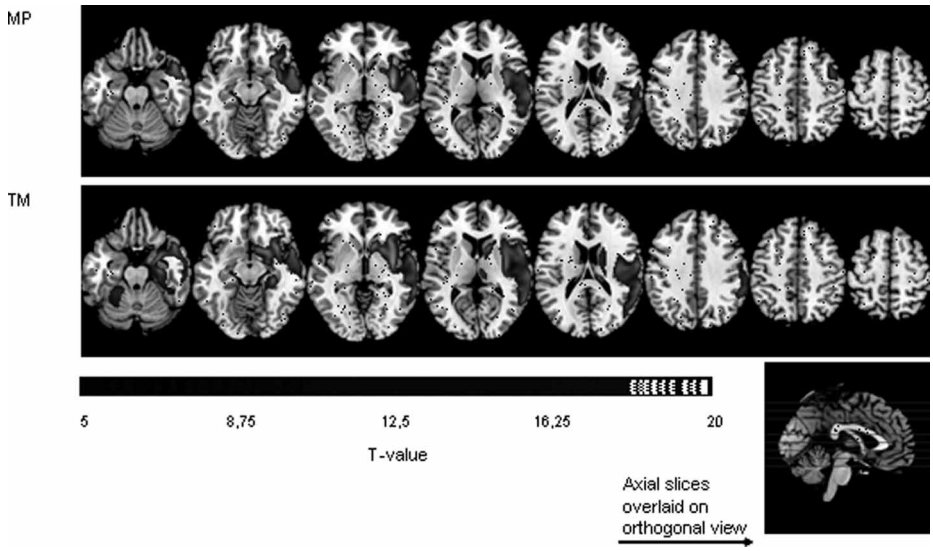

Figure 13. *Transcriptions of the lesions in patients M.P. and T.M. Lesion reconstructions in the patients from magnetic resonance imaging (MRI) scan. Lesions have been drawn in MRIcroN (Chris Rorden, 2007) onto ch2bet, a scalp-stripped version of the average of 27 T1-weighted scans from the same individual (displayed at www.bic.mni.mcgill.ca/cgi/icbm_view). The whole brain (right bottom) shows the 9 slices used. Left of the slice represents the left hemisphere.*

stimuli presented on each trial. The display began with a fixation cross (160 mm × 180 mm) for 500 ms, prior to the onset of the stimulus display. After that, the visual targets were presented on a black background on the computer screen using E-prime. The targets were the letters O (310 mm × 320 mm) and E (250 mm × 310 mm), which appeared 1° left or right of the fixation, viewed from about 60 cm.

Results

The data for the percentage of correct reports on 2-item trials are presented in Figure 14. Both patients scored 100% on single right trials (both 48/48). On single left trials M.P. scored 38/48 (79%) and T.M. 42/48 (87.5%). M.P. made 1 error on a 0-item trial (reporting a single left stimulus), and T.M. made 0 errors. Figure 14 indicates that 2-item reports tended to be better for identical conjunctions than for stimuli with 1 feature in common, and performance was worst when the stimuli had different features. Performance in the best 2-item condition was compared with the single left condition using a log linear analysis with the factors being patient, condition, and accuracy (number of correct and error trials). The best fitting model revealed an interaction between condition and accuracy: $\chi^2(4) = 1.30$, $p = .861$, for the model goodness of fit; $\chi^2(1) = 6.11$, $p < .025$, for the interaction between condition and accuracy. This indicates that accuracy was higher on single left trials even when compared with the best 2-item condition, across both patients. Thus there was an extinction effect.

Similar analyses were performed to assess differences between the 2-item trials. Neither patient showed a difference between the two types of 1-feature trial (same colour and shape identity), and therefore the data were pooled to create a single 1-feature condition. The contrast between performance with identical conjunctions and with 1 feature in common revealed a best fitting model with one interaction between condition and accuracy: $\chi^2\ (4) = 0.143$, $p = .998$, for the model goodness of fit; $\chi^2(1) = 17.68$, $p < .001$, for the interaction between condition and accuracy. The contrast between the 1-feature and the 0-feature conditions generated a similar

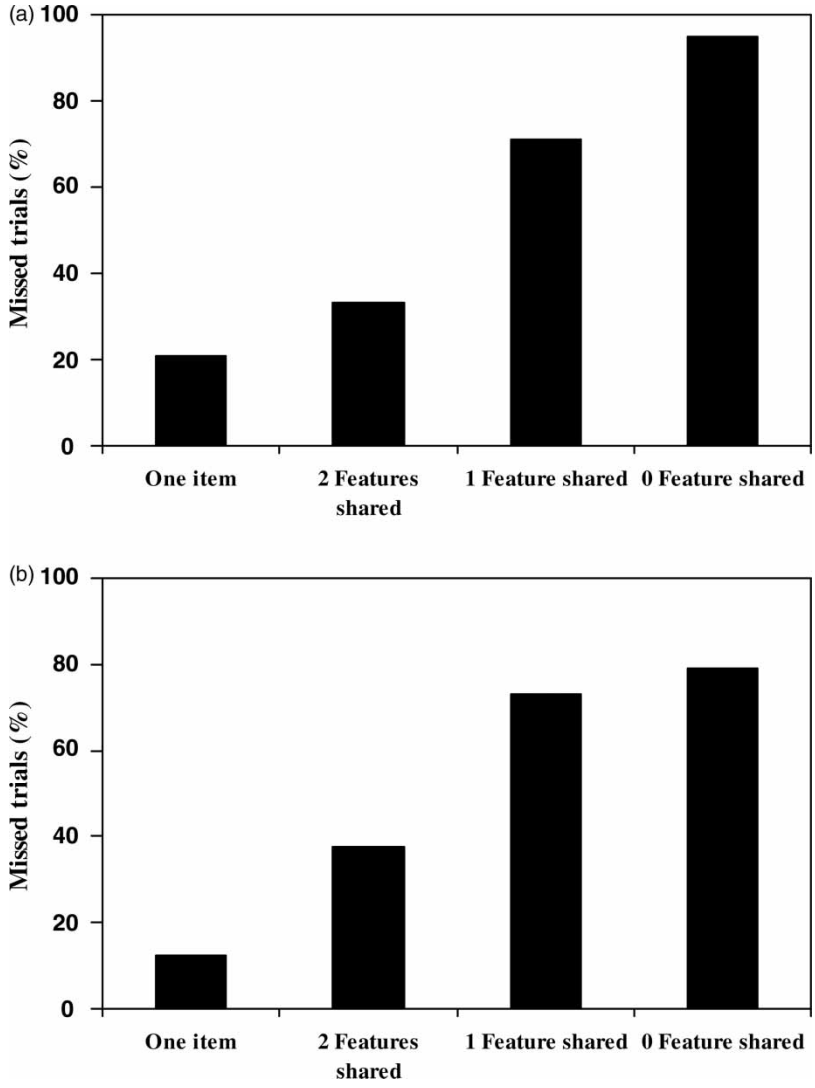

Figure 14. *Data from patients M.P. (a) and T.M. (b) when asked to report the presence of a 2, 1, or 0 stimulus (Experiment 1). For 2-item trials the colour and form relations between the stimuli were varied.*

result: $\chi^2(4) = 3.34$, $p = .502$, for the model goodness of fit; $\chi^2(1) = 4.78$, $p < .05$, for the interaction between condition and accuracy. These interactions indicate that proportionately more correct than error trials occurred in the identical conjunction condition than in the 1-feature condition, while there was also an advantage for the 1-feature condition over the 0-feature condition. These results held across both patients, though we note that T.M. showed only a minimal difference between the 1- and 0-feature conditions (Figure 14).

Discussion

The results indicate that there was a positive effect of similarity between the contra-and ipsilesional stimuli on performance. This result replicates

prior reports of recovery from extinction when patients are presented with visually similar items (e.g., Gilchrist et al., 1996; Humphreys, 1998). We note, however, that these data are in the opposite direction to results reported by Baylis and colleagues (1993, 2001), using similar stimuli. There are several potential important differences between the experiments. One is that we only required patients to report the presence of two stimuli while Baylis and colleagues asked patients to identify and localize the stimuli. The identification-and-localization task may require the establishment of separate token representations of the stimuli in VSTM, and a deficit at this level could lead to problems in registering the presence of 2 stimuli when the items share the critical to-be-reported feature. A second difference between the experiments is that we used a relatively small distance between the items while Baylis and colleagues (1993, 2001) employed large distances (12° from fixation). A small distance between the stimuli is likely to encourage perceptual interactions to take place (see Gilchrist et al., 1996, for evidence of distance effects on the positive effects of similarity on extinction), while large distances are likely to lead to the independent representation of the stimuli. Kitadono and Humphreys (2007) used a similar task to Baylis and colleagues and presented items at an intermediate distance (3° from fixation). They found no effects of similarity in either direction. It is possible that there was a balance between positive perceptual grouping between similar items on some trials, and impaired token representation of similar items on others, which on balance led to the null effect. Whichever the case, the data conform to the pattern predicted by sSoTS, in which detection of the contralesional stimuli is better when the items are identical than when they share either 1 or 0 features. sSoTS showed only a trend for a difference between the 1- and 0-feature conditions, a pattern similar to that with patient T.M. Whether there is a positive effect of a single shared feature between the stimuli may depend on individual differences in grouping strength. Interestingly, the advantage for identical conjunctions over items sharing a single feature indicates that the patients implicitly represented the conjunctive relationship between the colour and shape, given that similarity between the two conjunctions influenced extinction. Patients with PPC damage have been reported to be impaired at binding colour and shape representations (e.g., Cohen & Rafal, 1991; Friedman-Hill et al., 1995; Humphreys, Hodsoll, & Riddoch, 2009a), though there is also evidence for implicit conjunctive coding. For example, Wocjiulik and Kanwisher (1998) reported that patients could be sensitive to the colour–form relations in the Stroop colour-identification task, even when they could not explicitly report which colour was linked to one of two words (see also Cinel & Humphreys, 2006; Robertson, Treisman, Friedman-Hill, & Grabowecky, 1997, for converging evidence). Our results fit with this last pattern. sSoTS captures this pattern of implicit coding based on the coactivation of locations units by items with different features falling at the same position. The explicit binding of the features may require read-out from the feature maps following the feedback of activity from the location map, a process not currently implemented. This feedback and read-out process that may also be impaired after PPC damage (see Humphreys, 2001).

EXPERIMENT 2: EFFECTS OF THE TEMPORAL RELATIONS BETWEEN STIMULI

In the second empirical test of sSoTS we examined whether patients showing extinction manifested the particular pattern predicted by the model when the temporal relations between contra- and ipsilesional stimuli are varied. As in Simulation 5, we presented patients with 2-item trials in which the contralesional stimulus led, the ipsilesional stimulus led, or both stimuli occurred simultaneously. As in Experiment 1, the task was to report whether 0, 1, or 2 items appeared.

Method

T.M. and M.P. again both took part. We used stimuli that differed in both identity and shape

(O or E; red or green). There were 24 two-item trials in each presentation condition (contralesional first, simultaneous, ipsilesional first). There were also 72 one-item trials (36 left and 36 right) and 18 zero-item trials. For M.P. the stimuli were presented for 500 ms, and for T.M. they were presented for 350 ms (for each item, on sequential trials, and in total for the simultaneous condition—matching for the duration of each item). We also ran a final block of 24 trials in which we doubled the duration of the stimuli on two-item trials, to match the sequential and simultaneous conditions for the total duration of the items summed (as opposed to matching on the time available to process each item).

Results

The percentages of correct reports are given in Figure 15.

Neither patient made any errors on 0-item trials or on trials with a single right stimulus. T.M. scored 34/36 (94.4%) on single left trials and M.P. 31/36 (86.1%). Performance in the best 2-item condition (contralesional first) fell below the level found with single left stimuli (T.M.: 19/24, 79.2%; M.P.: 18/24, 75%). The data were analysed using a log linear analysis with the factors being patient, condition (single left vs. contralesional first) and accuracy (number correct or incorrect). This revealed a best fitting model in which there was an interaction between the stimulus condition and accuracy: $\chi^2(4) = 1.59$, $p = .812$, for the model goodness of fit; $\chi^2(1) = 3.85$, $p < .05$, for the interaction between condition and accuracy. Performance was relatively more accurate in the single left condition than the best 2-item condition.

Similar analyses were performed on the data in the different 2-item conditions. For the comparison between the contralesional first and ipsilesional first conditions, there was again a reliable interaction between condition and accuracy—$\chi^2(4) = 0.118$, $p = .998$, for the model goodness of fit; $\chi^2(1) = 7.74$, $p < .01$, for the interaction between condition and accuracy—demonstrating an advantage for the contralesional first condition. The ipsilesional first condition was then compared with the two simultaneous conditions. For the comparison with the simultaneous exposure matched to the duration of each stimulus, there was a Condition × Accuracy interaction: $\chi^2(4) = 1.14$, $p = .888$, for the model goodness of fit; $\chi^2(1) = 21.82$, $p < .001$, for the interaction between condition and accuracy. A similar pattern merged in the comparison when the simultaneous exposure matched the total duration of the sequential displays: $\chi^2(4) = 0.404$, $p = .982$ for the model goodness of fit; $\chi^2(1) = 4.40$, $p < .05$, for the interaction between condition and accuracy.

Discussion

The results found for T.M. and M.P. match those generated by sSoTS when lesioned. Report was overall better when the stimuli were presented consecutively than when they appeared concurrently, and this held both when the consecutive and simultaneous conditions were matched for the time to identify each item and when they were matched for overall presentation time. Our results here replicate findings reported by Baylis et al. (2002) and Di Pellegrino et al. (1997, 1998). Interestingly we also found that there was a benefit for the contralesional first condition compared with when the ipsilesional item led. This asymmetric pattern of performance is predicted by sSoTS. Previously, authors have reported that the lag between the stimuli needs to be longer to achieve accurate identification when the contralesional item leads than when the ipsilesional stimulus leads (Baylis et al., 2002). However, the prior studies have required target identification rather than detection, and this may involve higher level processes that are also impaired when items fall in the contralesional field. Under conditions of target detection, the tendency can be reversed.

GENERAL DISCUSSION

We have presented a spiking-level model of visual selection, sSoTS, whose parameters were set to

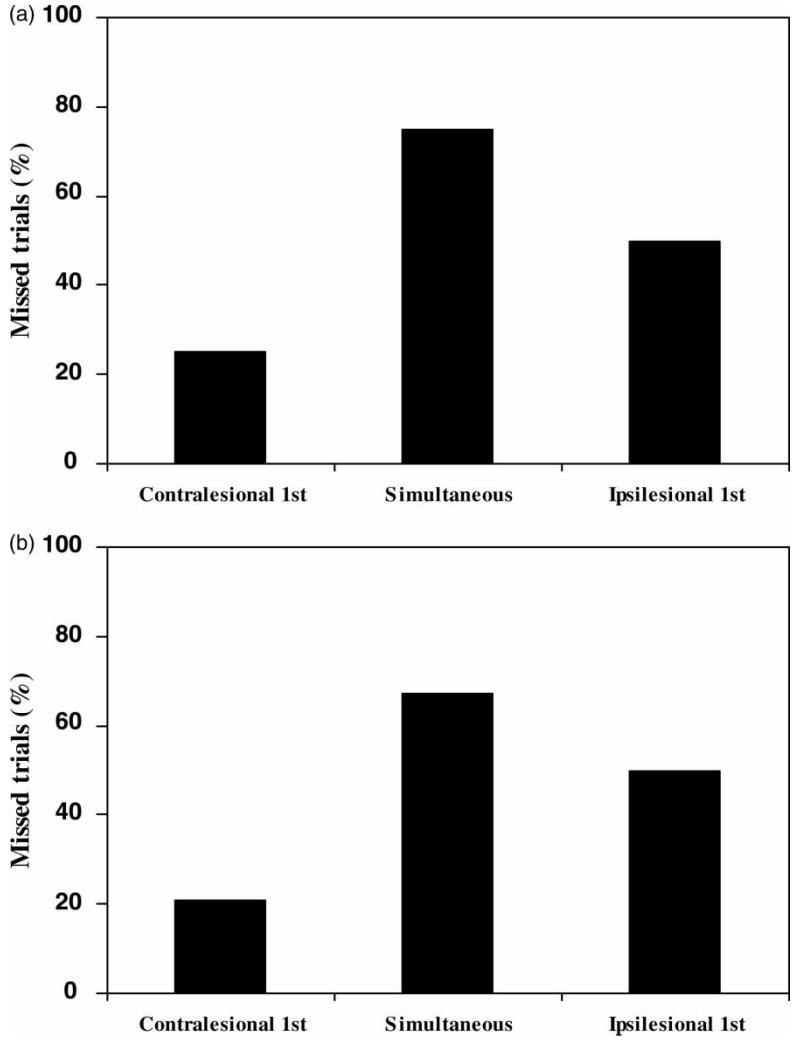

Figure 15. *Data from patients M.P. (a) and T.M. (b) when asked to report the presence of a 2, 1, or 0 stimulus (Experiment 2). Data here are from 2-item trials where the temporal relations between the stimulus were varied.*

match search efficiency in normal human observers. We then simulated the effects of unilateral damage to the PPC damage by unilaterally reducing the number of processing units on one side of the model's location map. We were able to simulate patterns of performance found in the neuropsychological literature, both for visual search performance (e.g., Olivers & Humphreys, 2004; Section 1) and for visual extinction with limited stimulus exposures (Section 2). We were also able to derive new predictions on the effect of visual similarity and temporal separation on visual extinction that were tested in patients (in Section 3). We discuss the data from each section in turn.

Section 1

There was clear evidence that conjunction search worsened relative to single-feature search, particularly for targets on the contralesional side. This

results has been reported in patients (Eglin et al., 1989; Friedman-Hill et al., 1995; Humphreys & Müller, 1993; Riddoch & Humphreys, 1987), where it has been interpreted as a deficit in binding features (e.g., Friedman-Hill et al., 1995). In sSoTS the deficit comes about not due to a specific binding deficit (indeed there is evidence for implicit binding after lesioning, based on the effects of stimulus similarity on performance; Simulation 4) but because there is more competition for selection in conjunction than with single-feature search. The effect of lesioning the model is to introduce noise into the competition for selection, disrupting performance in conditions where there is inherently more noise (in conjunction rather than single-feature search). The simulation provides an existence proof that a selective problem in conjunction compared with single-feature search is not necessarily due to poor binding. We believe this is the first simulation to demonstrate this.

There was also selective disruption to preview search compared with the single-feature baseline condition, even though search efficiency in these two conditions was matched for the unlesioned model. Hence the present result is not a simple case of the worse condition becoming even more difficult. An impairment in preview search has also been documented in PPC patients (Humphreys et al., 2006; Olivers & Humphreys, 2004). The deficit in preview search in the model comes about because of a variety of interacting factors, while, interestingly, factors critical to preview search in the unlesioned model were not damaged (frequency adaptation and top-down inhibition of old distractors). There was reduced activation for items on the contralesional side leading to a delay in the frequency adaptation process that normally contributed to old items being ignored. In addition, there was a delay on the accrual of activation for the new target falling in the contralesional field. In combination, these factors resulted in a reduced preview benefit in search, since old distractors remained available to compete with targets, and contralesional targets in particular were weaker competitors. The combined effects of these factors were demonstrated in Simulation 3 where we orthogonally varied the field where the old and the new items appeared. Similarly to Olivers and Humphreys (2004), we found that performance was best when the old and new stimuli appeared in opposite hemifields. For sSoTS this result occurred because (a) old items in the contralesional field were not strong competitors for new items in the ipsilesional field, and (b) old items in the ipsilesional field were subject to frequency adaptation by the time activation accrued for new, contralesional stimuli, so competition was reduced. The data contradict an account of preview search in terms of impaired disengagement of attention from ipsilesional stimuli. Prior accounts of deficits in preview search in PPC patients have argued for there being impaired spatio-temporal segmentation, but the exact mechanisms leading to this impairment have not been specified. sSoTS provides a first account of how visual selection mechanisms, when lesioned, may generate impaired spatio-temporal segmentation.

In addition to providing an existence proof of how spatio-temporal deficits in selection may arise independent of impaired visual binding, the simulations in Section 1 provided the first demonstration of how nonspatial deficits may arise after unilateral right PPC damage. Simulation 3 showed that down-regulation of a global neurotransmitter, affecting overall activation levels, exacerbated problems in spatial selection in the model while also introducing deficits for stimuli presented on the nonlesioned side. We suggest that this global change in the operation of the model mirrors the deficits associated with low arousal in patients (e.g., see Robertson & Manly, 1999). If we assume that right PPC damage selectively disrupts arousal by reducing excitatory neurotransmitter regulation (cf. Posner & Petersen, 1990), then these results can be linked to the greater spatial deficits found after right- than after left-PPC damage (arousal changing selectively after right-hemisphere lesions). As well as this, the lesions show that nonspatial deficits interact with the presence of a spatial bias in selection to worsen neglect in the model. There are interactive rather than additive relations between spatial biases in selection and arousal.

One other point concerns response variance. When lesioned, the variance of search increased for contralesional targets, with this increase being worse for conditions where noise was greater in the first place (for conjunction and preview search). This is an inherent property of models operating at a spiking level, where decreasing the processing units increases the noise present. The data match those from human patients (Figure 7).

Section 2

The simulations presented in Section 2 were designed to test for extinction (the magnitude of the lesion was lessened, and exposures durations were shortened). We showed that extinction in the model was sensitive to similarity relations between the features of ipsi- and contralesional stimuli (Simulation 4). Extinction was reduced when the ipsi- and contralesional items had the same combination of colour and shape, relative to when they differed in one or both features. This also indicates that performance was modulated by the conjunctive binding of colour and shape. In sSoTS the result occurred because there is reduced within-dimension competition when the ipsi- and contralesional stimuli are the same, compared with when they differ in at least one feature. Within-dimension competition is minimized when both features of the stimuli match. It would be interesting to add additional components to the model to enable it to group elements into larger perceptual objects and then to examine whether it can account for effects such as the influence of collinearity on extinction (Brooks et al., 2005; Gilchrist et al., 1996; Mattingley et al., 1997). For now, the data show that competitive interactions between stimuli are sufficient to generate positive effects of similarity on extinction.

These simulations with sSoTS contradict the data reported by Baylis and colleagues (1993, 2001), where patients showed greater extinction when stimuli matched on the dimension that determined perceptual report. We attribute this discrepancy to Baylis and colleagues (1993, 2001) presenting the stimuli at wide spatial separations and requiring patients to report the stimuli as separate tokens in VSTM. Deficits in identification and localization when items have the same feature may reflect an impairment at the level of VSTM. These aspects of performance are not simulated in sSoTS, which is more influenced by feature relationships in early perception.

The lesioned version of sSoTS was also influenced by the temporal relations between stimuli. Extinction was greatest when ipsi- and contralesional items appeared simultaneously relative to when they appeared across successive intervals, with performance being best when the contralesional item occurred first. The overall pattern of results (with performance worse under simultaneous than sequential presentation conditions) match data reported by Baylis et al. (2002) and Di Pellegrino et al. (1997, 1998), with the improved performance when the "contralesional" stimulus leads being a new prediction tested in Section 3.

The simulations in Section 2 confirm that extinction emerges from the competition for selection in sSoTS, and that specific effects of both featural and temporal relationships are predicted. In Section 3 we presented new data assessing the validity of these predictions.

Section 3

In Section 3 we reported two new experiments testing predictions from the simulations in Section 2. Experiment 1 replicated the effects of visual similarity on extinction, demonstrating sensitivity to implicit conjunctive coding in two patients. These results fit with previous data where positive effects of similarity have been reported on extinction patients (Gilchrist et al., 1996; Humphreys, 1998), though it has not been shown hitherto that benefits increase when stimuli have more features in common.

Experiment 2 tested performance with temporally staggered stimuli. Here we showed that, like sSoTS, neuropsychological patients produced better detection performance when a contralesional item leads rather than follows an ipsilesional stimulus. This last result contradicts the data

found by Baylis et al. (2002) and Di Pellegrino et al. (1997, 1998). We attribute this difference to the change between our use of a detection task and the prior use of identification tasks. We suggest that longer identification times are required for contralesional items. This can lead to poorer performance when the contralesional item leads because patients then switch to processing the ipsilesional stimuli prior to identification of the contralesional stimulus being completed. Whether or not this conjecture holds, however, our empirical results support the proposal from sSoTS that, when detection only is required, there is less perceptual competition for the contralesional stimulus when it is presented first.

Limitations and scope of the model

Although sSoTS can capture important aspects of human visual selection, and makes verifiable predictions, there are certainly limitations to the model. In particular, the neurons in sSDoTS are not linked directly to single cell recordings and they lack many of the physiological properties of neurons found in the brain regions relevant to human visual attention. For example, (a) the neurons in sSoTS do not have receptive field properties matched to those in ventral visual areas (the feature maps) or PPC (the location map) of the human cortex; (b) units in the feature maps respond in a highly specific way to the presence of critical features, not with the more graded tuning found in real neurons; (c) not all neurotransmitter systems are included (e.g., the NE system); (d) we simulate only two sets of features within each dimension and just six locations in the visual field; and (e) locations in the model are not really retinotopic, since the units within the pools at each position are not more strongly connected to neighbouring pools than to any other pools at other locations. Hence, at best, the simulations only provide a first approximation to human physiological responses. However, the simplifying assumptions we have made allow us to keep the complexity of the system to the minimum while capturing what we take to be important aspects of performance in a biologically plausible way (e.g., the time course of the build-up of calcium). Modelling is often a compromise between exact detail and generating simulations that generate emergent behaviour in reasonable computer running time and at a level of complexity we can match to behaviour. We believe that one interesting aspect of the present simulations is that they show that a model approximating operations within single neurons can both capture and predict behaviour at what we may term a "whole system" level (e.g., search times for targets). Through this modelling exercise, and through extending it in future work, we hope to provide a means of linking physiological operations to psychological function.

CONCLUSIONS

Overall, the data indicate that the sSoTS model can provide a powerful framework for integrating some of the different symptoms found after PPC damage—covering effects on serial search, on temporal selection, of reduced neurotransmitter modulation, and on extinction of visual similarity and the temporal relations between stimuli. In this respect, the model adds to other explicit simulations of neglect and extinction (Heinke & Humphreys, 2003; Mozer et al., 1997; Pouget & Sejnowski, 1997) while offering a first account of temporal as well as spatial aspects of performance and of response variance as well as mean performance levels. The model indicates how factors such as frequency adaptation may play an important role in visual selection, in addition to competitive and cooperative interactions between processing units. In addition, the simulations of neglect here point to the importance of interactions between different parts of the model in determining output. For example, activity in the feature maps as well as the location map were altered after lesioning only the location map, a result that arose because top-down interactivity was reduced. This follows the pattern found in patients with parietal lesions (Rees et al., 1990). This illustrates the importance of considering attentional

selection as an emergent property of interactions within a processing network.

In addition to contributing to our functional understanding of visual selection, sSoTS advances prior work on neglect by being more closely aligned than previous models to physiological properties of neural systems. As a consequence, sSoTS offers the possibility of a more detailed analysis than before of neuropsychological data in terms of the underlying neural pathology. An example of this here is provided by Simulation 3, where we evaluated the effects of reduced excitatory neurotransmitter operations and showed emerged deficits in selecting ipsi- as well as contralesional stimuli. sSoTS can provide a theoretical framework for such effects. It is also possible to use models such as sSoTS to predict the haemodynamic response function measured in fMRI experiments (Deco, Rolls, & Horwitz, 2004; Humphreys, Mavritsaki, Heinke, & Deco, 2009b), enabling the model to be tested using neural as well as behavioural data. An exciting possibility will be to examine changes in the haemodynamic response function after neural damage, to provide an account of structure–function relations in patients.

Manuscript received 22 October 2007
Revised manuscript received 29 June 2009
Revised manuscript accepted 20 October 2009

REFERENCES

Abeles, A. (1991). *Corticonics. Neural circuits of the cerebral cortex.* Cambridge, UK: Cambridge University Press.

Agter, A., & Donk, M. (2005). Prioritized selection in visual search through onset capture and color inhibition: Evidence from a probe-dot detection task. *Journal of Experimental Psychology: Human Perception and Performance*, *31*, 722–730.

Ahmed, B., Anderson, J., Douglas, R., Martin, K., & Whitteridge, D. (1998). Estimates of the net excitatory currents evoked by visual simulation of identified neurons in cat visual cortex. *Cerebral Cortex*, *8*, 462–476.

Allen, H. A., & Humphreys, G. W. (2007). A psychological investigation into the preview benefit in visual search. *Vision Research*, *47*, 735–745.

Anderson, G. M., Heinke, D. G., & Humphreys, G. W. (in press). Featural guidance in conjunction search: The contrast between orientation and color. *Journal of Experimental Psychology: Human Perception and Performance.*

Batelli, L., Cavanagh, P., & Thornton, I. M. (2003). Perception of biological motion in parietal patients. *Neuropsychologia*, *41*, 1808–1816.

Baylis, G. C., Driver, J., & Rafal, R. D. (1993). Visual extinction and stimulus repetition. *Journal of Cognitive Neuroscience*, *5*(4), 453–466.

Baylis, G. C., Gore, C. L., Rodriguez, P. D., & Shisler, R. J. (2001). Visual extinction and awareness: The importance of binding dorsal and ventral pathways. *Visual Cognition*, *8*, 359–379.

Baylis, G. C., Simon, S. L., Baylis, G. C., & Rorden, C. (2002). Visual extinction with double simultaneous stimulation: What is simultaneous? *Neuropsychologia*, *40*(7), 1027–1034.

Bisiach, E., & Vallar, E. (2000). Unilateral neglect in humans. In F. Boller & J. Grafman (Eds.), *Handbook of neurophysiology* (pp. 459–502). Amsterdam: Elsevier.

Braithwaite, J. J., & Humphreys, G. W. (2003). Inhibition and anticipation in visual search: Evidence from effects of color foreknowledge on preview search. *Perception & Psychophysics*, *65*, 213–237.

Braithwaite, J. J., Humphreys, G. W., & Hulleman, J. (2005). Color-based grouping and inhibition in visual search: Evidence from a probe-detection analysis of preview search. *Perception & Psychophysics*, *67*, 81–101.

Brooks, G. A., Fahey, T. D., & Kenneth, M. (2005). *Exercise physiology: Human bioenergetics and its applications.* Boston, MA: McGraw-Hill.

Brunel, N., & Wang, X. (2001). Effects of neuromodulation in a cortical networks model of object working memory dominated by current inhibition. *Journal of Computational Neuroscience*, *11*, 63–85.

Bundesen, C., Habekost, T., & Kyllingsbaek, S. (2005). A neural theory of visual attention: Bridging cognition and neurophysiology. *Psychological Review*, *112*, 291–328.

Cinel, C., & Humphreys, G. W. (2006). On the relations between implicit and explicit spatial binding: Evidence from Balint's syndrome. *Cognitive, Affective and Behavioral Neuroscience*, *6*(2), 127–140.

Cohen, A., & Rafal, R. D. (1991). Attention and feature integration—illusory conjunctions in a patient with a parietal lobe lesion. *Psychological Science*, *2*, 106–110.

Critchley, M. (1953). *The parietal lobes.* London: Edward Arnold.

Deco, G., & Rolls, E. (2005). Neurodynamics of biased competition and cooperation for attention: A model with spiking neuron. *Journal of Neurophysiology*, *94*, 295–313.

Deco, G., Rolls, E., & Horwitz, B. (2004). Integrating fMRI and single-cell data if visual working memory. *Neurocomputing*, *58/60*, 729–737.

Deco, G., & Zihl, J. (2001). Top-down selective visual attention: A neurodynamical approach. *Visual Cognition*, *8*(1), 119–140.

Di Pellegrino, G., Basso, G., & Frassinetti, F. (1997). Spatial extinction on double asynchronous stimulation. *Neuropsychologia*, *35*(9), 1215–1223.

Di Pellegrino, G., Basso, G., & Frassinetti, F. (1998). Visual extinction as a spatio-temporal disorder of selective attention. *Cognitive Neuroscience*, *9*(5), 835–839.

Duncan, J., Bundesen, C., Olson, A., Humphreys, G. W., Chavda, S., & Shibuya, H. (1999). Systematic analysis of deficits in visual attention. *Journal of Experimental Psychology*, *128*, 1–29.

Duncan, J., & Humphreys, G. W. (1989). Visual search and stimulus similarity. *Psychological Review*, *96*, 433–458.

Duncan, J., Humphreys, G. W., & Ward, R. (1997). Competitive brain activity in visual attention. *Current Opinion in Neurobiology*, *7*, 255–261.

Eglin, M., Robertson, L. C., & Rafal, R. D. (1989). Visual search performance in the neglect syndrome. *Journal of Cognitive Neuroscience*, *1*, 372–385.

Ellis, R., & Humphreys, G. W. (1999). *Connectionist psychology*. Hove, UK: Psychology Press.

Forti, S., & Humphreys, G. W. (2005). Cross-modal visuo-tactile matching in a patient with a semantic disorder. *Neuropsychologia*, *43*(11), 1568–1579.

Friedman-Hill, S. R., Robertson, L. C., & Treisman, A. (1995). Parietal contributions to visual feature binding—evidence from a patient with bilateral lesions. *Science*, *269*, 853–855.

Gilchrist, I., Humphreys, G. W., & Riddoch, M. J. (1996). Grouping and extinction: Evidence for low level modulation of selection. *Cognitive Neuropsychology*, *13*, 1223–1256.

Heinke, D., Deco, G., Zihl, J., & Humphreys, G. W. (2002). A computational neuroscience account of visual neglect. *Neurocomputing*, *44*, 811–816.

Heinke, D., & Humphreys, G. (2003). Attention, spatial representation and visual neglect: Simulating emergent attention and spatial memory in the selective attention for identification model (SAIM). *Psychological Review*, *110*, 29–87.

Hestrin, S., Sah, P., & Nicoll, R. (1990). Mechanisms generating the time course of dual component excitatory synaptic currents recorded in hippocampal slices. *Neuron*, *5*, 247–253.

Hodsoll, J., & Humphreys, G. W. (2001). Driving attention with the top down: The relative contribution of target templates to the linear separability effect in the size dimension. *Perception & Psychophysics*, *63*, 918–926.

Humphreys, G. (1998). Neural representation of objects in space: A dual coding account. *Philosophical Transactions of the Royal Society of London. Series B, Biological Sciences*, *353*, 1341–1351.

Humphreys, G. W. (2001). A multi-stage account of binding in vision: Neuropsychological evidence. *Visual Cognition*, *8*, 381–410.

Humphreys, G. W., Hodsoll, J., & Riddoch, M. J. (2009a). Fractionating the binding process: Neuropsychological evidence from reversed search efficiencies. *Journal of Experimental Psychology: Human Perception and Performance*, *35*, 627–647.

Humphreys, G. W., Jung Stalmann, B., & Olivers, C. N. L. (2004). An analysis of the time course of attention in preview search. *Perception and Psychophysics*, *66*(5), 713–730.

Humphreys, G. W., Mavritsaki, E., Heinke, D. G., & Deco, G. (2009b). Application of neural-level model to human visual search: Modelling the whole system behaviour, neuropsychological break down and BOLD signal activation. In D. G. Heinke & E. Mavritsaki (Eds.), *Bridging the gap between physiology and cognition*. Hove, UK: Psychology Press.

Humphreys, G. W., & Müller, H. J. (1993). SEarch via Recursive Rejection (SERR): A connectionist model of visual search. *Cognitive Psychology*, *25*, 43–110.

Humphreys, G. W., Olivers, C. N. L., & Braithwaite, J. J. (2006a). The time course of preview search with color-defined, not luminance-defined stimuli. *Perception & Psychophysics*, *68*(8), 1351–1358.

Humphreys, G. W., Olivers, C. N. L., & Yoon, E. Y. (2006b). An onset advantage without a preview benefit: Neuropsychological evidence separating onset and preview effects in search. *Journal of Cognitive Neuroscience*, *18*(1), 110–120.

Humphreys, G. W., & Price, C. J. (1994). Visual feature discrimination in simultanagnosia: A study of two cases. *Cognitive Neuropsychology*, *11*, 393–434.

Humphreys, G. W., & Riddoch, M. J. (1993). Interactions between object and space vision revealed through neuropsychology. In D. E. Meyer & S. Kornblum (Eds.), *Attention and Performance XIV*. Hillsdale, NJ: Lawrence Erlbaum Associates.

Humphreys, G. W., & Riddoch, M. J. (1994). Attention to within-object and between-object spatial representations: Multiple sites for visual selection. *Cognitive Neuropsychology*, *11*(2), 207.

Humphreys, G. W., & Riddoch, M. J. (1995). Separate coding of space within and between perceptual objects: Evidence from unilateral visual neglect. *Cognitive Neuropsychology*, *12*, 283–312.

Humphreys, G. W., Watelet, A., & Riddoch, M. J. (2006c). Long-term effects of prism adaptation in chronic visual neglect: A single case study. *Cognitive Neuropsychology*, *23*(3), 463–478.

Humphreys, G. W., Watson, D. G., & Joliceour, P. (2002). Fractionating visual marking: Dual task decomposition of the marking state by timing and modality. *Journal of Experimental Psychology: Human Perception and Performance*, *28*, 640–660.

Husain, M., Mannan, S., Hodgson, T., Wojciulik, E., Driver, J., & Kennard, C. (2001). Impaired spatial working memory across saccades contributes to abnormal search in parietal neglect. *Brain*, *124*(5), 941–952.

Husain, M., & Rorden, C. (2003). Non-spatially lateralized mechanisms in hemispatial neglect. *Nature Reviews. Neuroscience*, *4*, 26–36.

Husain, M., Shapiro, K., Martin, J., & Kennard, C. (1997). Abnormal temporal dynamics of visual attention in spatial neglect patients. *Nature*, *385*, 154–156.

Itti, L., & Koch, C. (2000). A saliency-based search mechanism for overt and covert shifts of visual attention. *Vision Research*, *40*, 1489–1506.

Jahr, C., & Stevens, C. (1990). Voltage-dependence of NMDA-activated macroscopic conductances predicted by single -channel kinetics. *Journal of Neuroscience*, *10*, 3178–3182.

Karnath, H. O. (1988). Deficits of attention in acute and recovered visual hemi-neglect. *Neuropsychologia*, *26*, 27–43.

Karnath, H. O., Himmelbach, M., & Kuker, W. (2003). The cortical substrate of visual extinction. *Neuroreport*, *14*, 437–442.

Kitadono, K., & Humphreys, G. W. (2007). Interaction between perception and action programming. *Cognitive Neuropsychology*, *24*, 731–754.

Kumada, T., & Humphreys, G. W. (2001). Lexical recovery from extinction: Interactions between visual form and stored knowledge modulate visual selection. *Cognitive Neuropsychology*, *18*(5), 465–478.

Ladavas, E., Petronio, A., & Umilta, C. (1990). The deployment of visual attention in the intact field of hemineglect patients. *Cortex*, *26*, 353–366.

Liu, Y., & Wang, X. (2001). Spike-frequency adaptation of a generalized leaky integrate-and-fire model neuron. *Journal of Computational Neuroscience*, *10*, 25–45.

Madison, D., & Nicoll, R. (1984). Control of the repetitive discharge of rate ca1 pyramidal neurons in vitro. *Journal of Physiology*, *345*, 319–331.

Malhotra, P., Parton, A. D., Greenwood, R., & Husain, M. (2005). Noradrenergic modulation of space exploration in visual neglect. *Annals of Neurology*, *59*, 186–190.

Mattingley, J. B., Davis, G., & Driver, J. (1997). Preattentive filling-in of visual surfaces in parietal extinction. *Science*, *275*, 671–674.

Mavritsaki, E., Heinke, D., Humphreys, G. W., & Deco, G. (2006). A computational model of visual marking using an interconnected network of spiking neurons: The spiking search over time & space model (sSoTS). *Journal of Physiology Paris*, *100*, 110–124.

Mavritsaki, E., Heinke, D., Humphreys, G., & Deco, G. (2007). Suppressive effects in visual search: A neurocomputational analysis of preview search. *Neurocomputing*.

McCormick, D., Connors, B., Loghthall, J., & Prince, D. (1985). Comparative electrophysiology of pyramidal and sparsely spiny stellate neurons in the neocortex. *Journal of Neurophysiology*, *54*, 782–806.

Mozer, M. C., & Behrmann, M. (1990). On the interaction of selective attention and lexical knowledge: A connectionist account of neglect dyslexia. *Journal of Cognitive Neuroscience*, *2*, 96–123.

Mozer, M. C., Halligan, P. W., & Marshall, J. C. (1997). The end of the line for a brain damaged model of unilateral neglect. *Journal of Cognitive Neuroscience*, *9*, 171–190.

Olivers, C., & Humphreys, G. W. (2002). When visual marking meets the attentional blink: More evidence for top-down limited capacity inhibition. *Journal of Experimental Psychology: Human Perception and Performance*, *28*, 22–42.

Olivers, C. N. L., & Humphreys, G. W. (2004). Spatiotemporal segregation in visual search: Evidence from parietal lesions. *Journal of Experimental Psychology*, *30*(4), 667–688.

Posner, M., & Cohen, Y. (1984). Components of visual orienting. In H. Bouma & D. Bouwhuis (Eds.), *Attention and Performance X: Control of language processes.* Hove, UK: Lawrence Erlbaum Associates.

Posner, M. I., & Petersen, S. E. (1990). The attention system of the human brain. *Annual Review of Neuroscience*, *13*, 25–42.

Pouget, A., & Sejnowski, T. J. (1997). A new view of hemineglect case on the response properties of parietal neurons. *Philosophical Transactions of the Royal Society of London. Series B, Biological Sciences*, *B352*, 1449–1459.

Rees, D., Backus, B., & Heeger, D. (2000). Activity in primary visual cortex predicts performance in a visual detection task. *Nature Neuroscience*, *3*, 940–945.

Riddoch, M. J., & Humphreys, G. W. (1987). Perceptual and action systems in unilateral neglect. In M. Jeannerod (Ed.), *Neurophysiological and neuropsychological aspects of spatial neglect.* Amsterdam: Elsevier Science.

Riddoch, M. J., Humphreys, G. W., Edwards, S., Baker, T., & Willson, K. (2003). Seeing the action: Neuropsychological evidence for action-based effects on object selection. *Nature Neuroscience*, *6*(1), 82–89.

Robertson, I. H. (1994). The rehabilitation of attentional and hemi-inattentional disorders. In M. J. Riddoch & G. W. Humphreys (Eds.), *Cognitive neuropsychology and cognitive rehabilitation* (pp. 173–186). Hove, UK: Lawrence Erlbaum Associates Ltd.

Robertson, I. H., & Manley, T. (1999). Sustained attention deficits in time and space. In G. W. Humphreys, J. Duncan, & A. Treisman (Eds.), *Attention, space and action: Studies in cognitive neuroscience* (pp. 279–310). Oxford, UK: Oxford University Press.

Robertson, I. H., Mattingley, J. B., Rorden, C., & Driver, J. (1998). Phasic alerting of neglect patients overcomes their spatial deficit in visual awareness. *Nature*, *396*(10), 169–172.

Robertson, L. C., Treisman, A., Friedman-Hill, S. R., & Grabowecky, M. (1997). The interaction of spatial and object pathways: Evidence from Balint's syndrome. *Journal of Cognitive Neuroscience*, *9*, 295–317.

Rolls, E., & Deco, G. (2002). *Computational neuroscience of vision*: Oxford, UK: Oxford University Press.

Rolls, E., & Treves, A. (1998). *Neural networks and brain function.* Oxford, UK: Oxford University Press.

Salin, P., & Prince, D. (1996). Spontaneous GABA-a receptor mediated inhibitory currents in adult rat somatosensory cortex. *Journal of Neurophysiology*, *75*, 1573–1588.

Seidenberg, M. S., & McClelland, J. L. (1989). A distributed, developmental model of word recognition and naming. *Psychological Review*, *96*(4), 523–568.

Sejnowski, T. J. (1986). Open questions about computation in cerebral cortex. In J. L. McClelland & D. E. Rumelhart (Ed.), *Parallel distributed processing: Psychological and biological models* (Vol. 2). Cambridge, MA: MIT Press.

Servan-Schreiber, D., Printz, H., & Cohen, J. D. (1990). A network model of catecholamine effects gain signal to noise ratio and behavior. *Science*, *249*(4971), 892–895.

Snow, J., & Mattingley, J. B. (2006). Goal-driven selective attention in patients with right hemisphere lesions: How intact is the ipsilesional field? *Brain Research Reviews*, *129*(1), 168–181.

Spruston, N., Jonas, P., & Sakmann, B. (1995). Dendritic glutamate receptor channel in rat hippocampal ca3 and ca1 pyramidal neurons. *Journal of Physiology*, *482*, 325–352.

Treisman, A., & Gelade, G. (1980). A feature-integration theory of attention. *Cognitive Psychology*, *12*, 97–136.

Tuckwell, H. (1998). *Introduction to theoretical neurobiology*. Cambridge, UK: Cambridge University Press.

Ward, R., Goodrich, S., & Driver, J. (1994). Grouping reduces visual extinction: Neuropsychological evidence for weight-linkage in visual selection. *Visual Cognition*, *1*, 101–130.

Watson, D., & Humphreys, G. (1997). Visual marking: Prioritizing selection for new objects by top-down attentional inhibition of old objects. *Psychological Review*, *104*, 90–122.

Watson, D., & Humphreys, G. (2000). Visual marking: Evidence for inhibition using probe-dot detection paradigm. *Perception and Psychophysics*, *62*, 471–480.

Watson, D., Humphreys, G., & Olivers, C. (2003). Visual marking: Using time in visual selection. *Trends in Cognitive Sciences*, *7*(4), 180–186.

Wilson, B. A., Cockburn, J., & Halligan, P. (1987). *The behavioral inattention test*. Bury St. Edmunds, UK: Thames Valley Test Company.

Wilson, F., O'Scalaidhe, S., & Goldman-Rakic, P. (1994). Functional synergism between putative gamma-aminobutyrate-containing neurons in

pyramidal neurons in prefrontal cortex. *Proceedings of the National Academy of Sciences*, *91*, 4009–4013.

Wojciulik, E., Husain, M., Clarke, K., & Driver, J. (2001). Spatial working memory deficit in unilateral neglect. *Neuropsychologia*, *39*, 390–396.

Wojciulik, E., & Kanwisher, N. (1998). Implicit visual attribute binding following bilateral parietal damage. *Visual Cognition*, *5*, 157–181.

Wolfe, J. W. (1994). Guided search 2.0: A revised model of visual search. *Psychonomic Bulletin and Review*, *1*(2), 202–238.

Xiang, Z., Huguenard, H., & Prince, D. (1998). GABA-a receptor mediated currents in interneurons and pyramidal cells of rat visual cortex. *Journal of Physiology*, *506*, 715–730.

APPENDIX A

In this appendix we present more details about the model of the spiking neurons used.

The subthreshold membrane potential of the neuron is given by the equation:

$$C_m \frac{dV(t)}{dt} = -g_m(V(t) - V_L) - I_{syn}(t) + I_{AHP}, \qquad 1$$

where C_m is the membrane capacitance, where different values are given for excitatory C_mex and inhibitory C_min neurons; g_m is the membrane leak conductance, where different values are also given for excitatory g_mex and inhibitory g_min neurons; V_L is the resting potential; I_{syn} is the synaptic current; and I_{AHP} is the current term for the frequency adaptation mechanism. The values for the above parameters as well as the threshold V_{tbr} and the reset potential (McCormick, Connors, Loghthall, & Prince, 1985) are given in Appendix C.

The synaptic currents used are described by the following equations.

The **AMPA** recurrent currents $I_{AMPA,rec}$ are given by:

$$I_{AMPA,rec}(t) = g_{AMPA,rec}(V(t) - V_E) \sum_{j=1}^{N_E} w_i s_j^{AMPA,rec}(t), \qquad 2$$

where V_E is the excitatory reversal potential, w_j are the synaptic weights, $g_{AMPA,rec}$ is the synaptic conductance, and $s_j^{AMPA,rec}$ is the receptors fraction of open channels.

The voltage of the **NMDA** recurrent currents $I_{NMDA,rec}$ is dependent on the extra-cellular magnesium $[Mg^{2+}]$ concentration (Jahr & Stevens, 1990):

$$I_{NMDA,rec}(t) = \frac{g_{NMDA}(V(t) - V_E)}{1 + [Mg^{2+}] \exp(-0.062V(t))/3.57} \times \sum_{j=1}^{N_E} w_j s_j^{NMDA}(t), \qquad 3$$

where $[Mg^{2+}]$ is the concentration of magnesium, g_{NMDA} is the synaptic conductance, and s_j^{NMDA} is the receptors fraction of open channels.

The voltage of the inhibitory **GABA** currents I_{GABA} is given by:

$$I_{GABA} = g_{GABA}(V(t) - V_I) \sum_{j=1}^{N_I} s_j^{GABA}(t), \qquad 4$$

where g_{GABA} is the synaptic conductance and s_j^{GABA} is the receptors fraction of open channels. The connections with the external neurons follow **AMPA**-like dynamics, and the voltage $I_{AMPA,ext}$ follows the following equation:

$$I_{AMPA,ext}(t) = g_{AMPA,ext}(V(t) - V_E) \sum_{j=1}^{N_{ext}} s_j^{AMPA,ext}(t), \qquad 5$$

where $g_{AMPA,ext}$ is the synaptic conductance and $s_{j=1}^{AMPA,ext}$ is the fraction of open channels. The parameters for Equations (2) to (5) are give in Appendix C. The synaptic current I_{syn} is given by the sum of the currents described above.

$$I_{syn}(t) = I_{AMPA,ext}(t) + I_{AMPA,rec}(t) + I_{NMDA,rec}(t) + I_{GABA}(t). \qquad 6$$

Furthermore, an additional current is added to the system that aims to simulate the frequency adaptation mechanism. The spike frequency adaptation mechanism used is based on $[Ca^{2+}]$- activated $[K^{+}]$ hyperpolarizing current I_{AHP} based on the assumption that this is the main current that produces this mechanism during the first 300 ms of adaptation (Madison & Nicoll, 1984). The I_{AHP} can be described by the equation:

$$I_{AHP}(t) = -g_{AHP}[Ca^{2+}](V(t) - V_K), \qquad 7$$

where V_K is the reversal potential of the K^{+} and g_{AHP} is the synaptic conductance. The mechanism for this current can be

described as the influx of a small amount of $[Ca^{2+}]$ α every time an action potential is generated; the intracellular level of $[Ca^{2+}]$ is thus increased, and this leads to further increment in I_{AHP}. The $[Ca^{2+}]$ between spikes can be described by the following equations:

$$\frac{d[Ca^{2+}]}{dt} = \frac{[Ca^{2+}]}{\tau_{Ca}} \quad 8$$

$$\text{if } V(t) = V_{thr}, \text{ then } [Ca^{2+}] = [Ca^{2+}] + a, \text{ and } V = V_{reset},$$

where ρ is the $[Ca^{2+}]$ influx and τ_{Ca} is the leaky integrator's decay constant. The $[Ca^{2+}]$ concentration is initially set to 0; the values for the rest of the parameters are given in Appendix C.

The open channel fractions are given by the following equations:

$$\frac{ds_j^{AMPA,rec}(t)}{dt} = -\frac{s_j^{AMPA,rec}(t)}{\tau_{AMPA}} + \sum_k \delta(t - t_j^k), \quad 9$$

where τ_{AMPA} is the decay time constant,

$$\frac{ds_j^{NMDA}(t)}{dt} = -\frac{s_j^{NMDA}(t)}{\tau_{NMDA,decay}} + ax_j(t)(1 - s_j^{NMDA}(t)), \quad 10$$

$$\frac{dx_j(t)}{dt} = -\frac{x_j(t)}{\tau_{NMDA,rise}} + \sum_k \delta(t - t_j^k), \quad 11$$

where $\tau_{NMDA,decay}$ is the decay time constant and $\tau_{NMDA,rise}$ is the rise time constant.

$$\frac{ds_j^{GABA}(t)}{dt} = -\frac{s_j^{GABA}(t)}{\tau_{GABA}} + \sum_k \delta(t - t_j^k), \quad 12$$

where τ_{GABA} is the decay time constant,

$$\frac{ds_j^{AMPA,ext}(t)}{dt} = -\frac{s_j^{AMPA,ext}(t)}{\tau_{AMPA}} + \sum_k \delta(t - t_j^k). \quad 13$$

The values for $\tau_{NMDA,rise}$, $\tau_{NMDA,decay}$, τ_{AMPA} (Hestrin, Sah, & Nicoll, 1990; Spruston, Jonas, & Sakmann, 1995), and τ_{GABA} (Salin & Prince, 1996; Xiang, Huguenard, & Prince, 1998) are given in Appendix C. The rise-time constants for AMPA and GABA are neglected because they are very small. Furthermore, it is considered that the spikes emitted from the presynaptic neuron j at time t_j^k are of the form of δ-peaks ($\delta(t)$).

APPENDIX B

This section introduces the reader to the mean field approximation as derived by Brunel and Wang (2001) and Deco and Rolls (2005). The mean field approximation is derived from the spiking neuron approach using a number of approximations (see Brunel & Wang, 2001; Deco & Rolls 2005). In order for this formulation to be used, it is assumed that the network of integrate-and-fire neurons is in a stationary state.

The potential of the neuron in the mean field is given by the equation:

$$\tau_x \frac{dV(t)}{dt} == V(t) + \mu_x + \sigma_x \sqrt{\tau_x}\eta(t), \quad 14$$

where μ_x is the mean value of the membrane potential in the absence of spiking and fluctuations, σ_x gives the magnitude of fluctuations, η is Gaussian process with time constant τ_{AMPA}, $V(x)$ is the membrane potential, x is the population of neurons, and τ_x is the membrane time constant. μ_x and σ_x^2 are given by the following equations:

$$\mu_x = \frac{(T_{ext}v_{ext} + T_{AMPA}n_x + \rho_1 N_x)V_E + \rho_2 N_x <V> + T_I w_{I,x} v_I V_I + V_L + (g_{AHP}[Ca^{2+}]_x V_K)/g_m}{S_x}, \quad 15$$

$$\sigma_x^2 = \frac{(g_{AMPA,ext}^2 v_{ext} + g_{AMPA,rec}^2 v_x) \times (<V> - V_E)^2 \tau_{AMPA}^2 \tau_x}{g_m^2 \tau_m^2}, \quad 16$$

where $w_{I,x}$ are the weights from the neurons in the inhibitory pools ($I = 1, \ldots, 3$) to the pool neurons in the pool x; v_I is the average spiking rate of the inhibitory pool I; $[Ca^{2+}]_x$ is the population average cytoplasmic $[Ca^{2+}]$ concentration; $\tau_m = C_m/g_m$, with different values depending on which pool is considered (excitatory or inhibitory); and v_{ext} is the external spiking rate as a summation of the spontaneous activity v_{sp}, external stimuli λ_{in}, and top-down attention λ_{att} with $v_{ext} = v_{sp} + \lambda_{in} + \lambda_{att}$. The rest of the quantities are given by the

following equations:

$$S_x = 1 + T_{ext}v_{ext} + T_{AMPA}n_x + (\rho_1 + \rho_2)N_x + T_I w_{I,x} v_I + \frac{g_{AHP}[Ca^{2+}]_x}{g_m}, \quad (17)$$

$$\tau_x = \frac{C_m}{g_m S_x}, \quad (18)$$

$$n_x = \sum_{j=1}^{n} f_j w_{j,x} v_j, \quad (19)$$

where ρ is the number of excitatory pools, f_x is the fraction of neurons in the x excitatory pool, and $w_{j,x}$ is the weight from pool j to pool x.

$$N_x = \sum_{j=1}^{p} f_j w_{j,x} \psi(v_j), \quad (20)$$

$$\psi(v) = \frac{v\tau_{NMDA}}{1 + v\tau_{NMDA}} \left(1 + \frac{1}{1 + v\tau_{NMDA}} \sum_{n=1}^{\infty} \frac{(-a\tau_{NMDA,rise})^n T_n(v)}{(n+1)!}\right), \quad (21)$$

$$T_n(v) = \sum_{k=0}^{n} (-1)^k \binom{n}{k} \times \frac{\tau_{NMDA,rise}(1 + v\tau_{NMDA})}{\tau_{NMDA,rise}(1 + v\tau_{NMDA}) + k\tau_{NMDA,decay}}, \quad (22)$$

$$\tau_{NMDA} = a\tau_{NMDA,rise}\tau_{NMDA,decay}, \quad (23)$$

$$T_{ext} = \frac{g_{AMPA,ext}C_{ext}\tau_{AMPA}}{g_m}, \quad (24)$$

$$T_{AMPA} = \frac{g_{AMPA,rec}N_E\tau_{AMPA}}{g_m}, \quad (25)$$

$$\rho_1 = \frac{g_{NMDA}N_E}{g_m J}, \quad (26)$$

$$\rho_2 = \beta \frac{g_{NMDA}N_E(<V> - V_E)(J-1)}{g_m J^2}, \quad (27)$$

where $\beta = 0.062$,

$$J = 1 + \gamma \exp(-\beta <V>), \quad (28)$$

where $\gamma = [Mg^{2+}]/3.5$ and $<V_x>$ has a value of between -55 mV and -50 mV,

$$T_I = \frac{g_{GABA}N_I\tau_{GABA}}{g_m}, \quad (29)$$

$$<V_x> = \mu_x - (V_{thr} - V_{reset})v_x\tau_x. \quad (30)$$

The following equations are solved numerically in parallel:

$$\tau_x \frac{dv_x}{dt} = -v_x + \phi(\mu_x, \sigma_x), \quad (31)$$

$$\tau_{Ca} \frac{d[Ca^{2+}]_x}{dt} = -[Ca^{2+}]_x + a\tau_{Ca}v_x, \quad (32)$$

where $v_x = \phi(\mu_x, \sigma_x)$ is the spiking rate of a pool as a function of the equations defined above, and

$$\phi(\mu_x, \sigma_x) = \left(\tau_{rp} + \tau_x \int_{\beta(\mu_x,\sigma_x)}^{a(\mu_x,\sigma_x)} du\sqrt{\pi}\exp(u^2)[1 + erf(u)]\right)^{-1}, \quad (33)$$

$$a(\mu_x, \sigma_x) = \frac{(V_{thr} - \mu_x)}{\sigma_x}\left(1 + 0.5\frac{\tau_{AMPA}}{\tau_x}\right) + 1.03\sqrt{\frac{\tau_{AMPA}}{\tau_x}} - 0.5\frac{\tau_{AMPA}}{\tau_x}, \quad (34)$$

$$\beta(\mu_x, \sigma_x) = \frac{(V_{reset} - \mu_x)}{\sigma_x}, \quad (35)$$

where *erf* is the error function and τ_{rp} the refractory period. The values for the parameters are shown in Appendix C.

APPENDIX C

Parameter values in sSoTs model

Parameters	*Values*	*Description*
C_m *excitatory*	0.2 nF	Membrane capacitance for excitatory neurons
C_m *inhibitory*	0.5 nF	Membrane capacitance for inhibitory neurons
g_m *excitatory*	25 nS	Membrane leak conductance for excitatory neurons
g_m *inhibitory*	20 nS	Membrane leak conductance for inhibitory neurons
V_L	− 70 mV	Resting membrane potential
V_E	0	Excitatory reversal potential
V_I	− 70 mV	Inhibitory reversal potential
V_{thr}	− 50 mV	Threshold membrane potential
V_{reset}	− 55 mV	Reset membrane potential
$g_{AMPA,rec}$ *excitatory*	0.104 nS	AMPA recurrent synaptic conductance for excitatory neurons
$g_{AMPA,rec}$ *inhibitory*	0.081 nS	AMPA recurrent synaptic conductance for inhibitory neurons
g_{NMDA} *excitatory*	0.22 nS	NMDA recurrent synaptic conductance for excitatory neurons
g_{NMDA} *inhibitory*	0.258 nS	NMDA recurrent synaptic conductance for inhibitory neurons
g_{GABA} *excitatory*	1.287 nS	GABA recurrent synaptic conductance for excitatory neurons
g_{GABA} *inhibitory*	1.002 nS	GABA recurrent synaptic conductance for inhibitory neurons
$g_{AMPA,ext}$ *excitatory*	2.08 nS	AMPA external synaptic conductance for excitatory neurons
$g_{AMPA,ext}$ *inhibitory*	1.62 nS	AMPA external synaptic conductance for inhibitory neurons
g_{AHP}	7.5 nS	$[Ca^{2+}]$-dependent K^+ channel synaptic conductance
τ_{AMPA}	2 ms	Decay time constant for AMPA
$\tau_{NMDA,decay}$	100 ms	Decay time constant for NMDA
$\tau_{NMDA,rise}$	2 ms	Rise time constant for NMDA
τ_{GABA}	10 ms	Decay time constant for GABA
τ_{Ca}	500 ms	Decay constant for leaky integrator
V_K	− 80 mV	Reversal potential for K^+ channel
a	0.15 μM	$[Ca^{2+}]$ influx when a spike occurs
N_E	1,600 (800)	Number of excitatory neurons in each layer for the feature maps (for the location map)
N_I	400 (200)	Number of inhibitory neurons in each layer for the feature maps (for the location map)
N_{ext}	800	Number of external neurons
τ_{rp} *inhibitory*	1 ms	Refractory period for inhibitory neurons
τ_{rp} *excitatory*	2 ms	Refractory period for excitatory neurons
$[Mg^{2+}]$	1 mM	Magnesium concentration
w^+	2.2	Coupling for the pools in the feature maps
w_{i1}	1.0	Inhibition for the two feature dimension maps
w_{i2}	0.9	Inhibition for the location map
w_{i3}	1.0	Connection weight from feature maps to location map
w_{i4}	0.25	Connection weight from the location map to feature maps
λ_{in}	120 Hz	The total input that each pool receives from the external neurons to show that there is an item in the visual field.
λ_{att}	185 Hz	The total top-down that the target pools receive to signify the target's characteristics.